

ULTRAVIOLET REFLECTIVITY AND BAND
STRUCTURE OF STANNIC OXIDE

By

BILL P. CLARK

Bachelor of Science
Oklahoma State University
Stillwater, Oklahoma
1961

Master of Science
Oklahoma State University
Stillwater, Oklahoma
1964

Submitted to the faculty of the Graduate College
of the Oklahoma State University
in partial fulfillment of the requirements
for the degree of
DOCTOR OF PHILOSOPHY
May, 1968

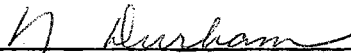
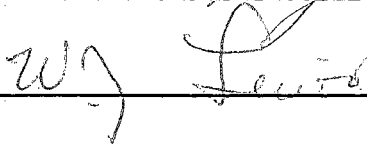
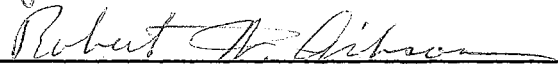

OCT 24 1968

ULTRAVIOLET REFLECTIVITY AND BAND
STRUCTURE OF STANNIC OXIDE

Thesis Approved:



Thesis Adviser



Dean of the Graduate College

688258

ACKNOWLEDGMENT

There have been many people responsible for the execution of the problem to be discussed. In particular, a note of thanks is offered Dr. E. E. Kohnke for suggesting the problem and supplying many interesting and fruitful suggestions and discussions regarding the project and its ultimate goals.

Similarly, H. Hall, and the other members of the Physics and Chemistry Shop of Oklahoma State University, deserve recognition for their aid in designing the monochromator as well as for doing an exceptional job in its construction.

During the early stages of the problem, J. Rutledge and J. Tunheim offered many helpful suggestions regarding different aspects of the experimental and theoretical work respectively. A particular note of thanks is extended P. Bower and F. Hajek for a significant amount of aid during the early stages of the programming required to solve the eigenvalue problem by machine.

Of course, this project could not have been attempted if it weren't for financial aid. Such aid came from a number of sources and was invaluable. In this respect, Dr. H. E. Harrington, Head of the Physics Department of Oklahoma State University, is to be thanked for the assistantship used during the earliest period of graduate work. Major financial support was furnished by The Office of Naval Research in sponsoring the project of which this was one part.

TABLE OF CONTENTS

Chapter	Page
I. INTRODUCTION.	1
II. OPTICAL PROPERTIES OF MATERIALS	3
III. OPTICAL MEASUREMENTS.	10
The Monochromator.	10
Samples and Their Surface Preparation.	21
Reflectivity Results	23
IV. GENERAL BAND THEORY FORMALISM	27
V. THE CALCULATION	39
VI. DISCUSSION OF RESULTS	61
VII. SUGGESTIONS FOR FURTHER STUDY	68
BIBLIOGRAPHY.	70
APPENDIX A. SINGLE GROUP ANALYSIS.	74
APPENDIX B. DOUBLE GROUP ANALYSIS AND TIME REVERSAL.	83
APPENDIX C. OPTICAL SELECTION RULES.	94

LIST OF TABLES

Table	Page
I. Oxygen Form Factor Parameters.	41
II. D_{14} Character System	48
III. Substitutions for D_{14}^{4h}	49
IV. Application of Space Group Operations to (1,1,1) Wave- functions.	51
V. Stannic Oxide Wavefunctions.	53
VI. Diamond Wavefunctions.	53
VII. Free Electron Energy Eigenvalues and Their Corresponding Symmetrized Combinations of Plane Waves.	56
VIII. Classes and Wave Vector Group Elements at Γ , A, M, Z, X, R, Λ , U, W, S, Σ , Δ , V, Y, T.	75
IX. Characters at Γ	77
X. Characters at A.	78
XI. Characters at M.	79
XII. Character System at X and R.	80
XIII. Character System for the Point Λ	80
XIV. Character System at S, Σ , Δ , and Y	80
XV. Representation Applicable at U, W, and T	81
XVI. Allowed Representations at V	81
XVII. Compatibility Relations.	82
XVIII. Double Group Irreducible Representations at Γ	85
XIX. Additional Representations at Γ	86
XX. Additional Representations at A and Z.	86

LIST OF TABLES (CONT'D)

Table	Page
XXI. Additional Representations at Λ	87
XXII. Additional Representations at Δ	87
XXIII. Additional Representations at W, U, and T	87
XXIV. Additional Representations at S, Σ , and Y.	88
XXV. Additional Representations and Double Group Elements at X	89
XXVI. Additional Representations and Double Group Classes at R	90
XXVII. Additional Representations and Double Group Classes at M	91
XXVIII. Additional Representations and Double Group Classes at V	93
XXIX. Compatible Electronic States (Double Group)	93
XXX. Optical Selection Rules at Γ	97
XXXI. Possible Allowed Transitions.	98
XXXII. Possible Allowed Transitions at Δ	98
XXXIII. Possible Allowed Transitions at Λ	99

LIST OF FIGURES

Figure	Page
1. The Monochromator.	11
2. The Grating Chamber.	12
3. The Entrance Slit.	15
4. The Detection Chamber.	16
5. The Sample Holder and Phototube.	18
6. Calibration Plots Using Some Prominant Lines of the Mercury Spectrum	20
7. Reflectance vs Energy for Natural Cassiterite ($\vec{E} \perp c$).	24
8. Reflectance vs Energy for a Vapor-Grown Stannic Oxide Single Crystal.	25
9. Initial Oxygen Form Factor	43
10. Initial Tin Form Factor	44
11. Final Tin and Oxygen Form Factors Used in the Calculation.	45
12. Factored (111) Secular Equation for the Stannic Oxide Structure	54
13. Factored (111) Secular Equation for the Diamond Structure.	55
14. Schematic Representation of the Factored Secular Equation Applicable to the Stannic Oxide Structure Using Nineteen Plane Waves.	57
15. Components of the Secular Equation Illustrated in Figure 14.	58
16. Pseudopotential Energy Bands Along the Axis $\Gamma-\Delta-X$	100

CHAPTER I

INTRODUCTION

Stannic Oxide is a member of the crystal system D_{4h}^{14} . A number of previous studies of the electrical and optical properties of this material have been reported (1-6). However, as yet, no attempt to correlate the available data via a band structure calculation using the one electron theory of solids has been made available. Such a study would attempt to predict mathematically some of the gross electrical and optical properties of the material in question from existing self-consistent data for the free atoms which make up the material. This type of "first principles" calculation has as its basic problem the mathematical formulation of the potential which will be seen by an electron as it traverses the real crystal lattice. However, the selection of a proper potential can be made through the usual self-consistent routine. Although a sufficient amount of data for a first principles band structure calculation is now available, prior calculations of this type on other systems have been shown to be of sufficient error to warrant another approach for a preliminary investigation. As a first step, then it has been decided to make an empirical pseudopotential calculation to test the general applicability of the one electron approximation for explaining experimental data, and to act as a guide for future theoretical calculations of a more fundamental nature.

Since the study of the reflectance spectrum of a crystal for light

of energy larger than the band gap has proven to be of significant value in treating metals and other materials in which the one electron theory has been applied, it was felt that following the work of Van Hove (7), Phillips (8), Brust (9), and many others might prove to be of particular value in attempting to obtain further optical properties of stannic oxide which would lead to a better understanding of the type and strength of force seen by an electron within the lattice as it moves from one energy state to another.

In this sense, the calculation should augment the experimental data and vice versa. The attempt to make the calculation self-consistent involves adjusting the pseudopotential parameters until as many of these measured quantities as possible may be predicted by the results of the calculation. After this situation has been optimized, it should be possible to infer the type of potential seen by an electron as it moves through the lattice by Fourier transformation of the final pseudopotential used.

To summarize, the problem under study involves three parts, 1) determination of the optical reflectance for light of energy greater than that of the band gap, 2) utilization of the empirical pseudopotential formulation and other data in a first attempt to describe a band structure for stannic oxide, and finally, 3) correlation of the reflectance spectrum and the calculated bands.

CHAPTER II

OPTICAL PROPERTIES OF MATERIALS

A complete treatment of the optical properties of solids is beyond the scope of this paper. The reader who is interested in the many theoretical implications and mathematical descriptions of such optical properties is referred to several excellent review articles and texts available on this topic (10,11,12,13,14,15,16,17,18).

A general mathematical treatment of the optical properties of materials can have its basis in the theory of propagation of electromagnetic waves in conducting media. This theory will be briefly reviewed below following Moss (12).

When considering the propagation of electromagnetic waves in conducting materials it is necessary to begin with the Maxwell equations which for this case have the form:

$$\vec{\nabla} \times \vec{E} = -\mu \mu_0 \frac{\partial \vec{H}}{\partial t} \quad (1)$$

$$\vec{\nabla} \times \vec{H} = \vec{J} + \epsilon \epsilon_0 \frac{\partial \vec{E}}{\partial t} \quad (2)$$

$$\vec{\nabla} \cdot \vec{H} = 0 \quad (3)$$

$$\vec{\nabla} \cdot \vec{E} = 0 \quad (4)$$

where

ϵ_0 = dielectric permittivity of free space

μ_0 = permeability of free space

ϵ = specific dielectric constant

μ = specific permeability

σ = electrical conductivity.

Taking the curl of equations (1) and (2) and applying the identity

$\nabla \times \nabla \times \vec{A} = \nabla(\nabla \cdot \vec{A}) - \nabla^2 \vec{A}$ it is possible to obtain:

$$\nabla^2 \vec{E} = \mu \mu_0 \left(\nabla \frac{\partial \vec{E}}{\partial t} + \epsilon \epsilon_0 \frac{\partial^2 \vec{E}}{\partial t^2} \right) \quad (5)$$

$$\nabla^2 \vec{H} = -\mu \mu_0 \left(\nabla \frac{\partial \vec{H}}{\partial t} + \epsilon \epsilon_0 \frac{\partial^2 \vec{H}}{\partial t^2} \right) \quad (6)$$

The solution of one component of these equations may be written as:

$$\vec{U}_x = \vec{U}_0 e^{i(t-x/v)} \text{ where } \vec{U} \text{ can stand for } \vec{E} \text{ or } \vec{H}. \quad (7)$$

This implies that

$$1/v^2 = \mu_0 \epsilon_0 \mu \epsilon - i \nabla \mu \mu_0 / \omega. \quad (8)$$

However,

$$v = c/N \quad (9)$$

where c = velocity of light and N is the refractive index of the medium.

Equation (8) may be therefore rewritten in the form

$$N^2 = c^2 \mu_0 \epsilon_0 \left\{ \mu \epsilon - i \frac{\nabla \mu}{\epsilon_0 \omega} \right\}, \quad (10)$$

and if the conductivity is nonzero the index of refraction must be complex and of the form

$$N = n - ik. \quad (11)$$

This changes the form of Equation (7) to

$$U_x = U_0 e^{i\omega t} e^{-i\omega n x/c} e^{-\omega k x/c} \quad (12)$$

with

$$n^2 - k^2 = \mu\epsilon \text{ and } 2nk = \sigma\mu/\omega\epsilon_0. \quad (13)$$

For cases of practical interest, $\mu = 1$, which implies that

$$2n^2 = \epsilon \left\{ 1 + \left(1 + \sigma^2/\omega^2\epsilon^2\epsilon_0^2 \right)^{1/2} \right\} \quad (14)$$

$$2k^2 = \epsilon \left\{ 1 - \left(1 + \sigma^2/\omega^2\epsilon^2\epsilon_0^2 \right)^{1/2} \right\}. \quad (15)$$

At this point it should be noted that σ is the conductivity of the medium at the optical frequency concerned rather than the dc or low frequency conductivity. As such, it contains any and all loss mechanisms which may arise at any frequency.

The absorption coefficient K is defined by the condition that the energy carried by the wave drops by a factor of e in a distance $1/K$. Since energy flow is given by the Poynting vector, K is proportional to the product of amplitudes of electric and magnetic field vectors. Both of these contain the term $e^{-\omega k x/c}$ as an attenuation factor. Thus the total attenuation in a distance x is given by $e^{-2\omega k x/c}$ which implies that K and k are related by

$$K = 2\omega k/c = 4\pi k/\lambda. \quad (16)$$

The next problem to be considered involves the behavior of an electromagnetic wave as it strikes a surface. In this case, Snell's and Fresnel's laws are still valid. However, their interpretation is complicated by the fact that the angle of refraction is sometimes imaginary

and, in the refracted wave, planes of constant phase and constant amplitude no longer coincide. The treatment of this problem for any angle of incidence is given in detail by Stratton (18) and is quite lengthy since many boundary conditions must be stated, the wave must be broken up into components with polarizations parallel and perpendicular to the plane of incidence, each component must satisfy the Maxwell equations with the proper boundary conditions, and then Snell's law must be invoked to obtain a reflectance and transmittance dependent upon the angle of incidence. Such procedure when followed for both the electric field and magnetic field vectors results in general expressions for angle-dependent reflectance and transmittance which reduce to the following simple forms in the case of normal incidence:

$$R = \frac{(n_2 - n_1)^2}{(n_2 + n_1)^2} \quad (17)$$

$$T = \frac{4n_1n_2}{(n_2 + n_1)^2} \quad (18)$$

where R is the reflectance, T is the transmittance, and n_1 and n_2 are the refractive indices of mediums one and two, respectively.

If the medium containing the incident wave is air ($n_1 = 1.0$) and the second medium has a complex index of refraction given by

$$n_2 = n - ik, \quad (19)$$

the reflectance, reflection coefficient, (or as it is called here) the reflectivity, may be written as:

$$R = \frac{(n - ik - 1)^2}{(n - ik + 1)^2} = \frac{(n - 1)^2 + k^2}{(n + 1)^2 + k^2}. \quad (20)$$

Following Stern (19), this reflectivity relation may in principle be used in conjunction with the relation between the extinction coefficient k and the absorption coefficient K to classify the possible electronic transitions by studying the absorption coefficient of the material in question, extracting the slope of the absorption coefficient curve as a function of energy, and from this slope, determining the density of states of the material as well as its energy-dependent refractive index. However, Stern noted that due to the lack of appreciable structure in the absorption curve, a treatment based upon measurements of the absorption alone is insufficient for a comprehensive study of the important electronic transitions.

The problem itself is not insoluble, however, since other workers in this area (20,21,22,23,24) have indicated that many details of the electronic band structure in different types of solids can be obtained by critically studying the structure of the imaginary part of the complex dielectric constant ($2nk$) which is related experimentally to the reflectance of the material being investigated. Philipp and Taft (25) have shown that the real and imaginary parts of the refractive index (n and k) can be obtained from the reflectivity spectrum at normal incidence by calculating the integral

$$\theta(E_0) = \frac{1}{2\pi} \int_0^{\infty} \frac{d \ln R(E)}{dE} \ln \left| \frac{E + E_0}{E - E_0} \right| dE. \quad (21)$$

Then n and k are given as the solution of the equation

$$\frac{n - ik - 1}{n - ik + 1} = R^{\frac{1}{2}} e^{i\theta}. \quad (22)$$

Thus with reflectance data on hand as a function of energy it is in prin-

principle possible to determine all of the optical constants of a material simply by applying this argument to the data acquired at normal incidence. Such Kramers-Kronig analysis (Equation 21) of reflectance spectra have been carried out in several investigations (20,21,22,25,26,28). However, as pointed out by Phillips (10) there is often less than 0.4 electron volt difference in the energy location of the observed reflectance peaks and the $2nk$ peaks using values of n and k obtained as above.

The analytic singularities in the $2nk$ curve acquired via a Kramers-Kronig analysis of the material's reflectance also show a correlation with those of the joint density-of-states function

$$\frac{d N_{ij}}{dE} = \int_{S_k} \frac{d S_k}{|\vec{\nabla}_k E_{ij}|} \quad (23)$$

where

$$E_{ij} = E_i(k) - E_j(k)$$

is the energy difference between conduction and valence band states and the domain of integration covers constant momentum surfaces. Thus the same conclusions regarding singularities may be drawn simply by investigating the structure of the acquired reflectance spectrum. This effect of singularities in the joint density-of-states due to $|\vec{\nabla}_k E_{ij}|$ being zero has been studied in detail by Van Hove (7) and Phillips (18) and is quite amenable to further application regarding the optical-electrical properties of solids.

Many other workers have used the aforementioned methods to study the optical properties of solids (27,28,29,30). For a complete and comprehensive listing of the references on this matter, the reader is re-

ferred to the review articles by Phillips (1) and Lax (27).

Another point noted by Phillips, Ehrenreich, and Philipp (33) and again by Phillips (34), is that a wide range of data indicates that the ultraviolet structure in the reflectance curve depends primarily on crystal structure and only secondarily on atomic composition. The characteristic structure of ultraviolet absorption is assigned to interband transitions that are applicable at symmetry points of the Brillouin zone, and just as the energy bands of materials seem to show some sort of consistent trend (35,36) for a given space group, the reflectance from any set of crystals with the same crystal structure appears to be somewhat alike. If these observations are coupled with the facts that anisotropic crystals have polarization-dependent reflectivities and that the reflectance of rutile has been acquired by Cardona and Harbeke (37), a plan of attack to be followed in studying the optical properties of stannic oxide becomes apparent.

This plan is preliminary in nature and rather elementary in content at this time, but appears to be consistent with the type of optical investigation that has been carried out for many other materials in a particular crystal class. The problem to be considered theoretically and experimentally involves acquiring some idea of the reflectance of stannic oxide as a function of the incident photon energy, comparing this data with that of rutile (when polarization measurements are possible), calculating a tentative band structure in which the symmetry of the initial and final electron states may be classified, and as a future problem, noting if such a trend of reproducibility in both the optical reflectance data and the band structures of materials having this type of crystal structure is evident.

CHAPTER III

OPTICAL MEASUREMENTS

The Monochromator

The reflectivity measurements were obtained using an instrument built in the Chemistry-Physics Shop at Oklahoma State University. Although several features of existing systems of this type were considered (38,39), an attempt was made to integrate the best features of the most favored system into a single instrument of flexibility sufficient for studies in several different regions of the optical spectrum.

Figure 1 shows the monochromator in perspective. Upon viewing this figure, it may be seen that the system consists of three distinct parts, sample chamber, grating chamber, and entrance & exit tubes. This fact may be used to advantage for later work in that should the sample chamber need modification, it may be easily removed. Similarly, the grating chamber may be altered, and the slit-to-grating distance may be increased simply by the insertion of the proper length tubes or tube sections. The entire system was electroless nickel plated by the Kaningen process to avoid erosion.

The grating chamber (Fig. 2) was constructed from a steel tube of fourteen-inch diameter and length of six inches. At the base of this chamber is an exit tube which connects to an oil diffusion pump. The top and bottom plates which are fastened to the grating chamber have been sealed using O-rings in order to insure keeping the chamber light

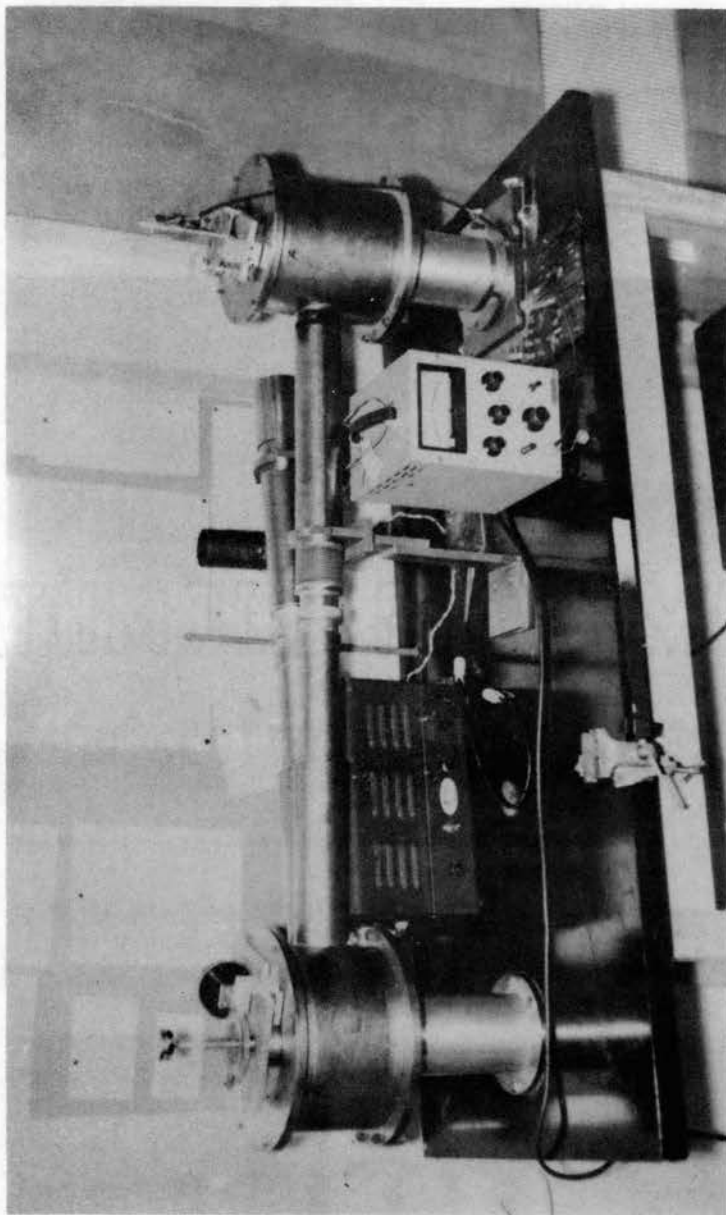


Figure 1. The Monochromator

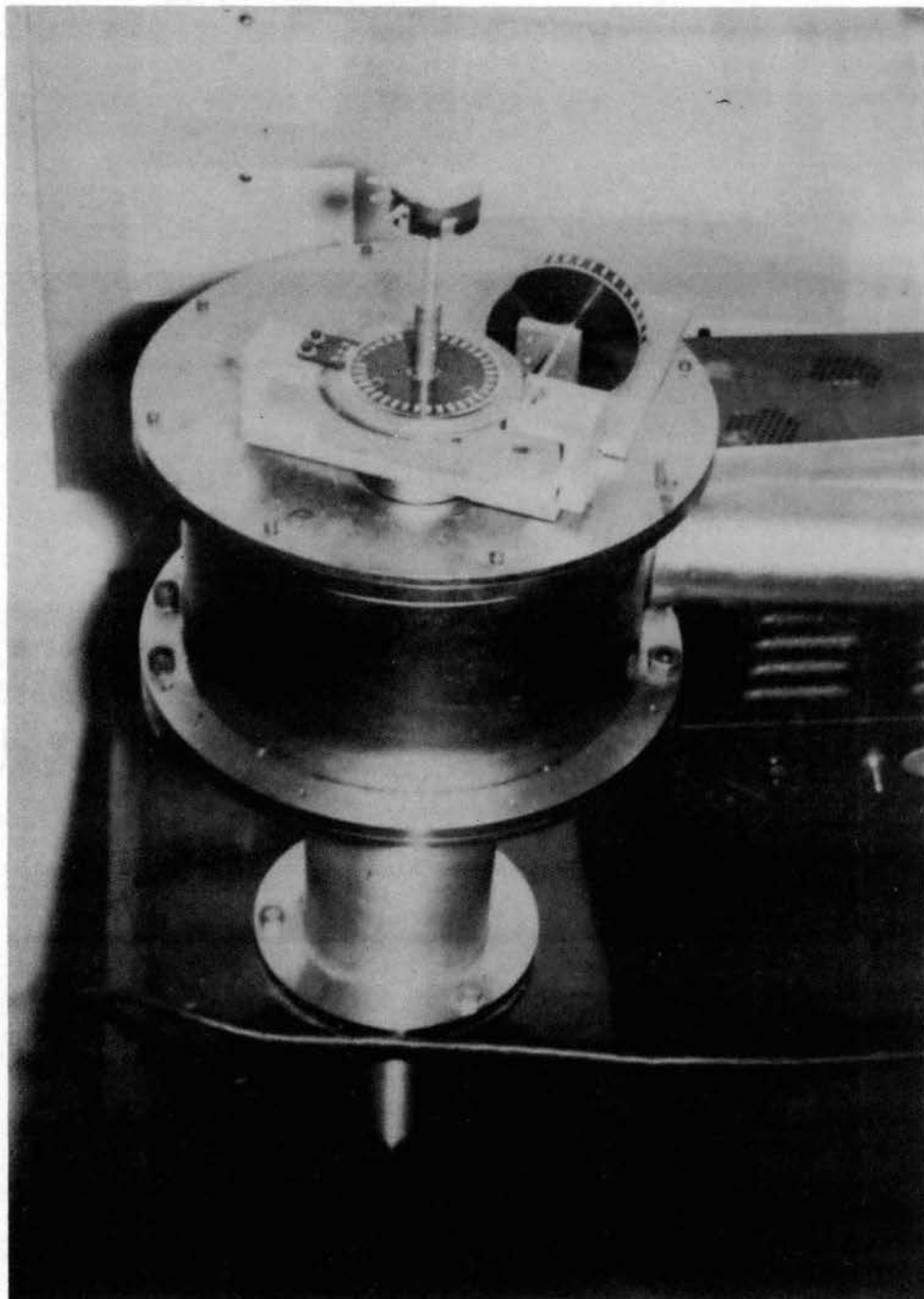


Figure 2. The Grating Chamber

tight as well as allowing for vacuum measurements. The grating used was a Bausch and Lomb replica "CP" grating with 6000 lines/cm which was blazed for 2760 angstroms at normal incidence. This grating was mounted using an off-center pivot similar to that discussed by Johnson (40). As pointed out by Johnson, the utilization of such a grating mount allows perfect focus for two different wavelengths in the first order and a near-perfect focus with deviation of less than two per cent for the wavelengths between the two focused wavelengths selected. For this system it was felt that perfect focus would be desirable at a wavelength which corresponds to the approximate energy of the intrinsic band gap of the material being studied. Thus, the off-center pivot was constructed in such a way as to allow perfect focus at 2260 angstroms and 3260 angstroms.

The relative position of the grating may be determined by reading the angle on the horizontal vernier scale shown in Figure 2. The vertical vernier moves through an angle of 180 degrees for every degree on the horizontal scale. Thus, assuming no backlash, the grating may be placed at any predetermined angle with respect to the entrance beam with an accuracy of twenty seconds of arc as read on the horizontal scale. However, upon propagating the error for such a setting experimentally, it was found that there was indeed some backlash in the gearing mechanism. This error was not found to be serious since data were taken by sweeping out the entire spectrum rather than going to one point in the spectrum, backing up to another point, and then proceeding to a point past the initial one. Also, it was felt that the data acquired were good since the backlash could be virtually eliminated by turning the grating through an angle of 100 degrees on the vertical scale past that

used for the last data point, then returning to that point and sweeping out the spectrum in the opposite direction.

The entrance and exit tubes were made in sections as may be seen from Figure 1. This was done to increase the flexibility of the system in that should conditions warrant changing gratings, any larger Rowland circle may be used simply by inserting sections of tubing of the proper length.

The entrance slit is shown in Figure 3. This slit may be aligned in two ways. Other than adjusting the slit width and its orientation relative to the ruled surface of the grating, it is also possible to adjust the slit-to-grating distance via rotation of the section containing the slit which has been attached by threads to the entrance tube.

The detection chamber is shown in greater detail in Figure 4. This chamber was made to be flexible in that the entire system is sealed to the exit tube by a double O-ring arrangement. This allows vacuum measurements without welding the exit tube to the chamber. The chamber itself was constructed of a tube at diameter 12 inches and length of fifteen inches. As was the case for the grating chamber, this tube is sealed to its top and bottom covers by an O-ring arrangement. The detection chamber is supported by a tube which rests on a stage as shown in Figure 1. This stage rests on 4 ball bearings placed in grooves in the base plate. Thus, the system may be moved in any direction in the plane of the table upon which the base plate is fastened, and locked into position by tightening the screws which make contact with the sides of the plate which supports the detection chamber. Such an elaborate arrangement turned out to be unnecessary for alignment of the slit with respect to the exit tube but could prove to be of significant value for

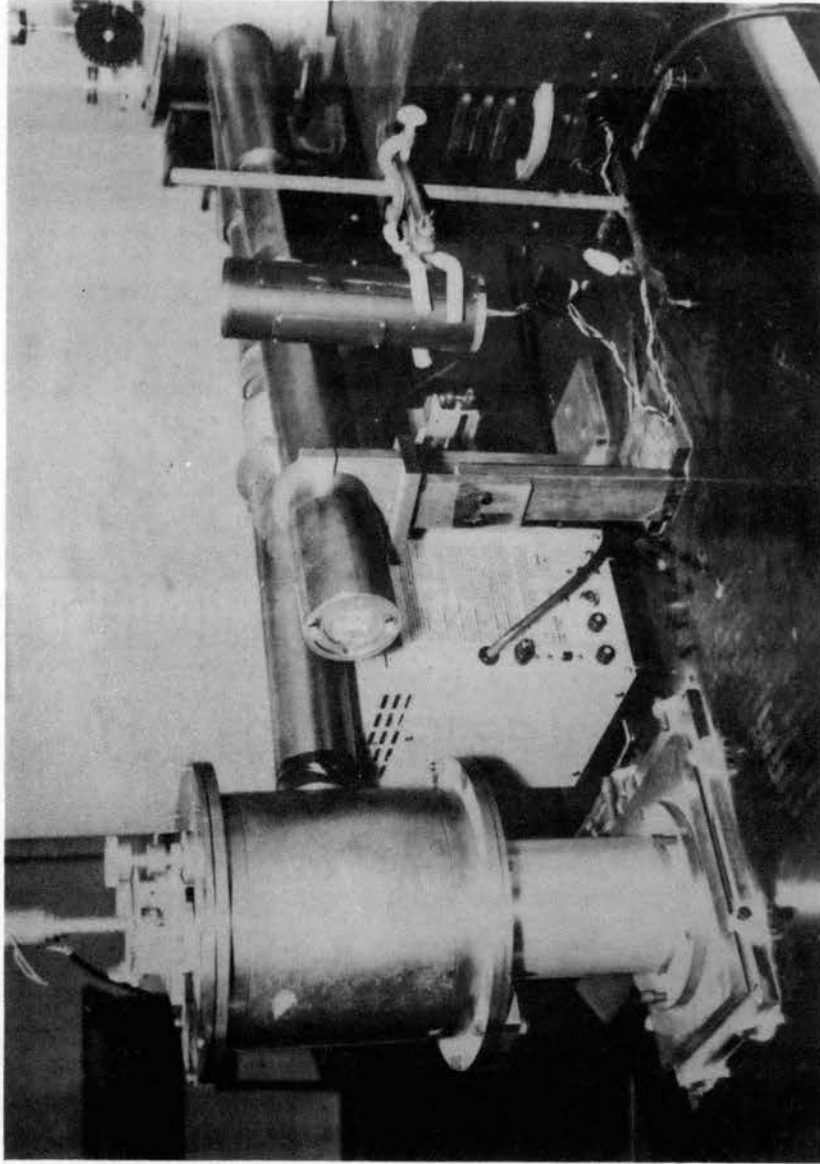


Figure 3. The Entrance Slit

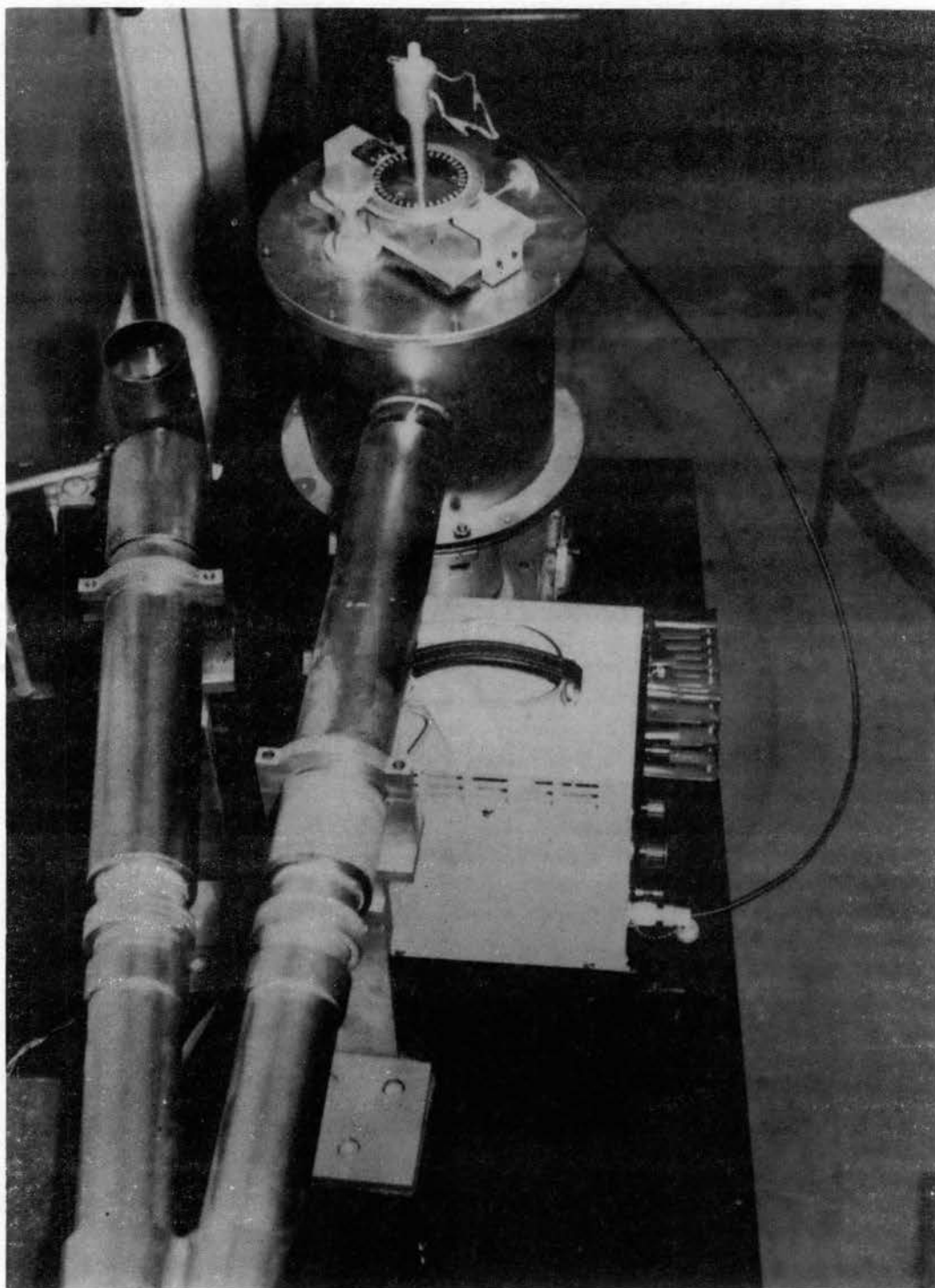


Figure 4. The Detection Chamber

future use if it were found that the detection chamber was not aligned properly with respect to the geometric center of the exit tube.

Only one detector was used (RCA phototube type 1P28) throughout the course of the experiment and its location inside the detection chamber is quite important. This is true since the most desirable situation is one wherein the optical path from the exit slit to the detector may at all times be considered to be constant. If this be the case, the actual magnitude of the reflectivity may be ascertained from relative measurements by using an argument based solely upon the geometry of the system. For this reason, the detector was mounted through the center of the top plate of the detection chamber in such a manner that it could be rotated to any position within the chamber. The relative position of the detector could be readily ascertained by reading the vernier scale which was mounted upon its shaft. The sample was mounted so that it could be rotated in and out of the beam using the knob shown in Figure 5, which also shows the phototube, sample holder, and sample in inverted position.

As has been noted by others (41,42), phototubes such as the RCA 1P28 which do not have an appreciable spectral response in the ultraviolet region of the spectrum may be made sensitive to radiation in this region by spraying the glass envelope of the tube with a solution of sodium salicylate in methanol. The complete details of the procedures for preparing a phototube in this manner are presented by Allison, Burns, and Tuzzolino (42). Briefly, the ultraviolet sensitivity arises due to the ability of the sodium salicylate to absorb radiation in this spectral range and then reemit light at 4300 angstroms with a quantum efficiency of nearly 100%. This latter being the region of greatest spectral sensitivity for this tube allows measurements to be made

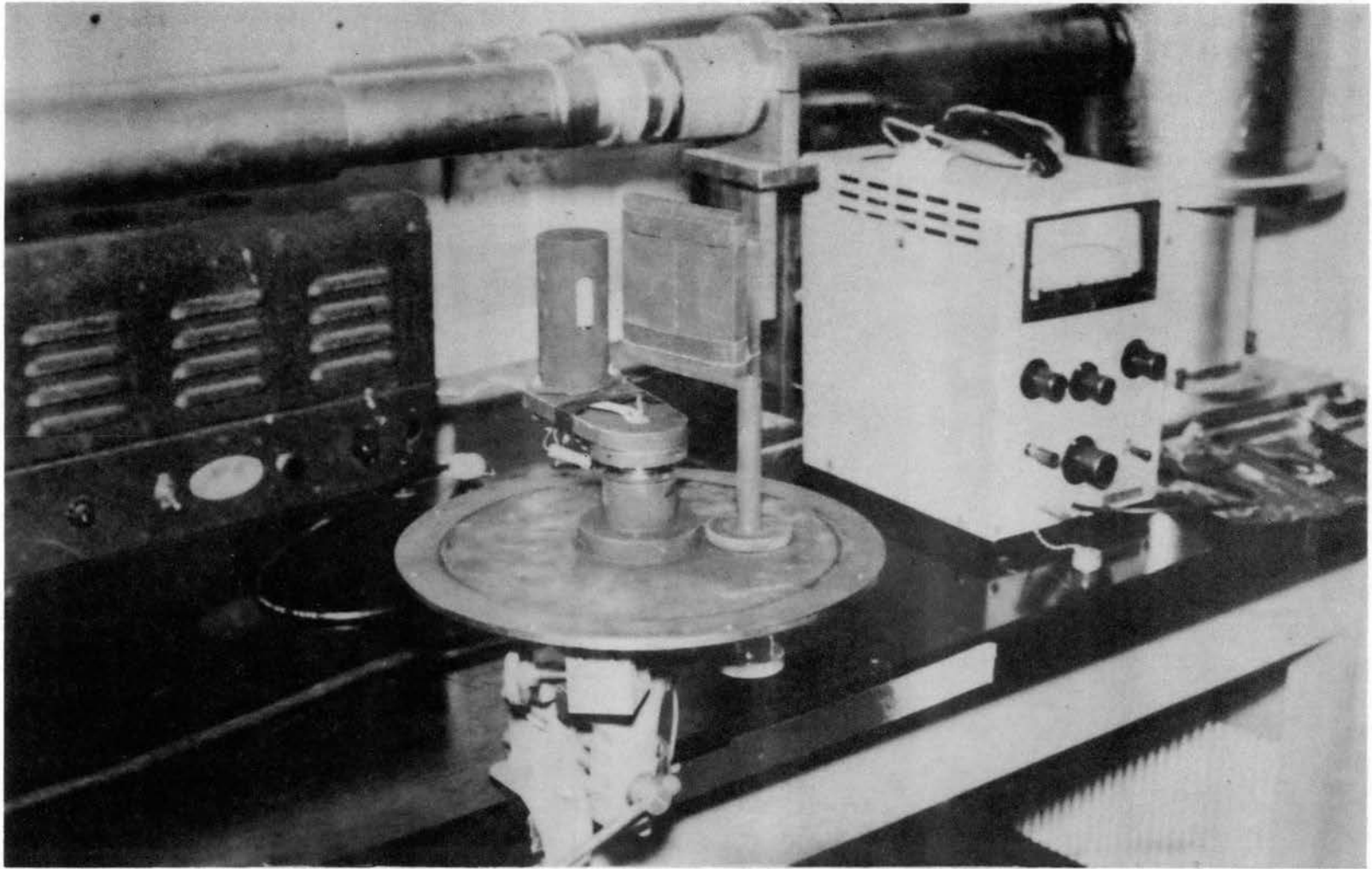


Figure 5. The Sample Holder and Phototube

inexpensively while yielding a means of determining the output intensity of any source of ultraviolet radiation.

Several different light sources were used at various stages of the experimental work. For purposes of calibration a mercury arc (Osram Hg3 Spectral Lamp) was used. However, this source is unsatisfactory for wavelengths below 2000 angstroms and due to its giving a line spectrum with very little overlap between lines, it is unsatisfactory for scanning a rather large range of energy in a continuous fashion. This necessitated the use of a light source which had a continuous spectrum in the region of interest with an intensity sufficient for the work desired. For this reason the preliminary measurements were made using a hydrogen arc. Hydrogen has a continuous spectrum in this wavelength range and was satisfactory for this purpose. A deuterium lamp (type OSRAM D102-S) was used extensively throughout the latter stages of the experiment. This lamp is roughly three to four times brighter than the hydrogen lamp. For future work a hydrogen discharge arc following Phillip and Ehrenrich (6) has been built which should increase both the spectral range covered and the intensity of the output radiation.

The apparatus was calibrated approximately by using the output of a Bausch and Lomb (Serial No. RD82) monochromator as the input source of radiation. After roughly locating the mercury lines, the Bausch and Lomb instrument was replaced by the mercury arc and the lines were then located carefully. The resulting calibration plot is shown in Figure 6. In this figure, the first line, L_1 , represents the initial calibration plot while the second line, L_2 , represents the calibration plot currently being used. It was necessary to re-calibrate when the grating was removed and then re-inserted into the system. At the time, it was sus-

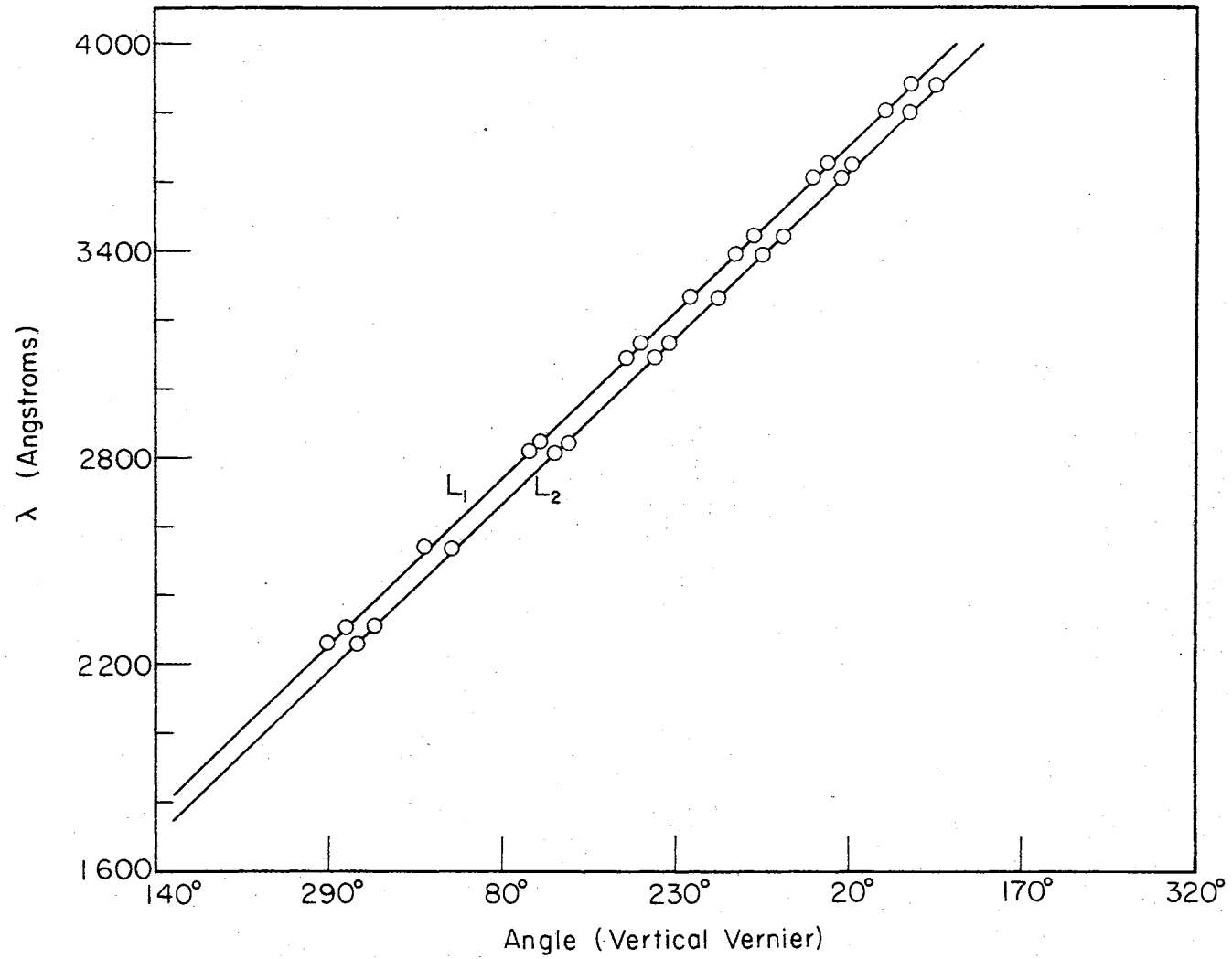


Figure 6. Calibration Plots Using Some Prominent Lines of the Mercury Spectrum

pected that if the 2536 angstrom line were found for the second case, the new calibration plot would simply be a line parallel to the first yet passing through this point. That such is the case is easily verified by inspection of Figure 6.

In an attempt to further check the calibration and become acquainted with the system, measurements of the reflectivity of single crystal silicon were made. The reflectance spectrum of the silicon was then compared with that of Ehrenreich and Philipp (43). Since the spectrum obtained agreed with their data, further confidence was gained as to the accuracy of the final calibration plot and the method of measurement.

After checking the spectrum of silicon, several attempts were made to measure the reflectivity of stannic oxide. Although a number of natural samples of Bolivian cassiterite were available, only one of these was used. Phillip (10,34) has noted that for non-cubic materials there should be differences in the reflectance spectra for light incident parallel and perpendicular to their optic axes. The one sample used was the only sample of Bolivian cassiterite available which had been cut so the optic axis was well defined with respect to the sample surfaces. The reflectance spectrum of synthetic stannic oxide was also desired for comparison but was quite difficult to obtain due to the small size of the crystals on hand. For this reason, this spectrum was ultimately measured using a vapor-grown crystal furnished by Corning Glass Works. The results of these measurements are illustrated in Figures 7 and 8.

Samples and Their Surface Preparation

As mentioned above, this work was carried out using two types of

stannic oxide samples. The natural cassiterite sample has the form of a triangular prism and was cut from one-half of a twin specimen in such a manner that the c-axis is perpendicular to the triangular faces. For further discussion about the optical properties and the method of cutting this prism the reader is referred to the M.S. Thesis cited as reference (44).

The other sample was furnished by Corning Glass Works and prepared by a vapor deposition technique. This crystal was used in preference to one grown by Kunkle and Kohnke (45) simply because of its larger surface area. The c-axis lies along its length, it is of 1 mm^2 cross section, and has a length of 2 cm. Thus comparison between the data acquired for this crystal and for the cassiterite specimen must be made very carefully due to the difference in orientation of the c-axes in the two instances.

A standard cleansing procedure for these crystals was adopted in order to assure reproducibility from one set of data to the next. This is extremely important since it has been shown (46) that certain aspects of the reflectance spectrum may vanish and then reappear if a crystal is first cleansed and then allowed to become contaminated.

The insolubility of stannic oxide in acids led to a method of cleaning the crystal in five steps as has been mentioned by Kunkle (47). This method was used when dealing with the electrical properties of stannic oxide and was felt to be adequate for a study of its optical properties. The procedure is given below:

- 1) four hours in aqua regia
- 2) four hours in hydrofluoric acid
- 3) rinse (acetone)

- 4) rinse (methanol)
- 5) rinse (distilled water).

The times given are not truly representative of the various cleaning procedures used since when the crystals were extremely dirty and did not exhibit a reflectance spectrum that could be immediately reproduced, they had to be placed in the acids for periods of days or even weeks before reproducible data was again obtained.

Reflectivity Results

For the purposes of this work the most important difference between the stannic oxide crystals used is in the orientations of their optic axes with the plane of the incident radiation.

The data shown in Figure 7 were obtained for the natural sample while those of Figure 8 were acquired for the grown sample. The current output of the phototube was read with a Keithley 610B electrometer for reflected light and also for light that was simply transmitted from the slit (exit) to the phototube with the sample out of the beam. The ratio of the currents measured at each point of the spectrum of interest yields the relative reflectance of the sample being studied in a direct manner.

After acquiring the reflectance versus energy curve for each sample a number of times, the data was normalized to yield the curves indicated in Figures 7 and 8. For this normalization the energy of five electron volts was taken as reference and at this point the reflectance was considered to have a magnitude of 100 in arbitrary units. In this manner, each curve could be drawn with reference to the others and any deviations in shape or position of reflectivity noted immediately.

As expected, the two sample types exhibit a difference reflectance

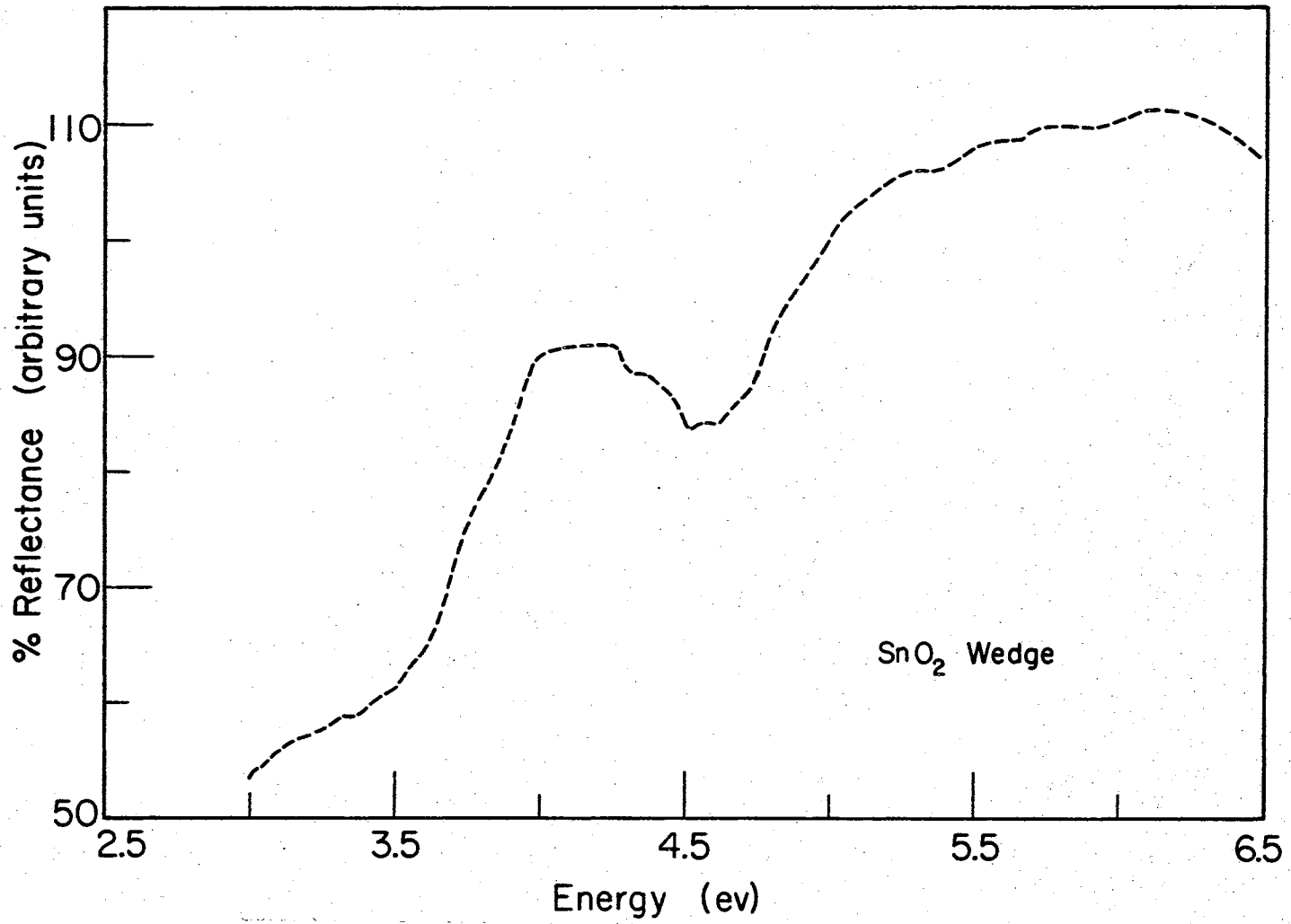


Figure 7. Reflectance vs Energy for Natural Cassiterite ($\vec{E} \perp c$)

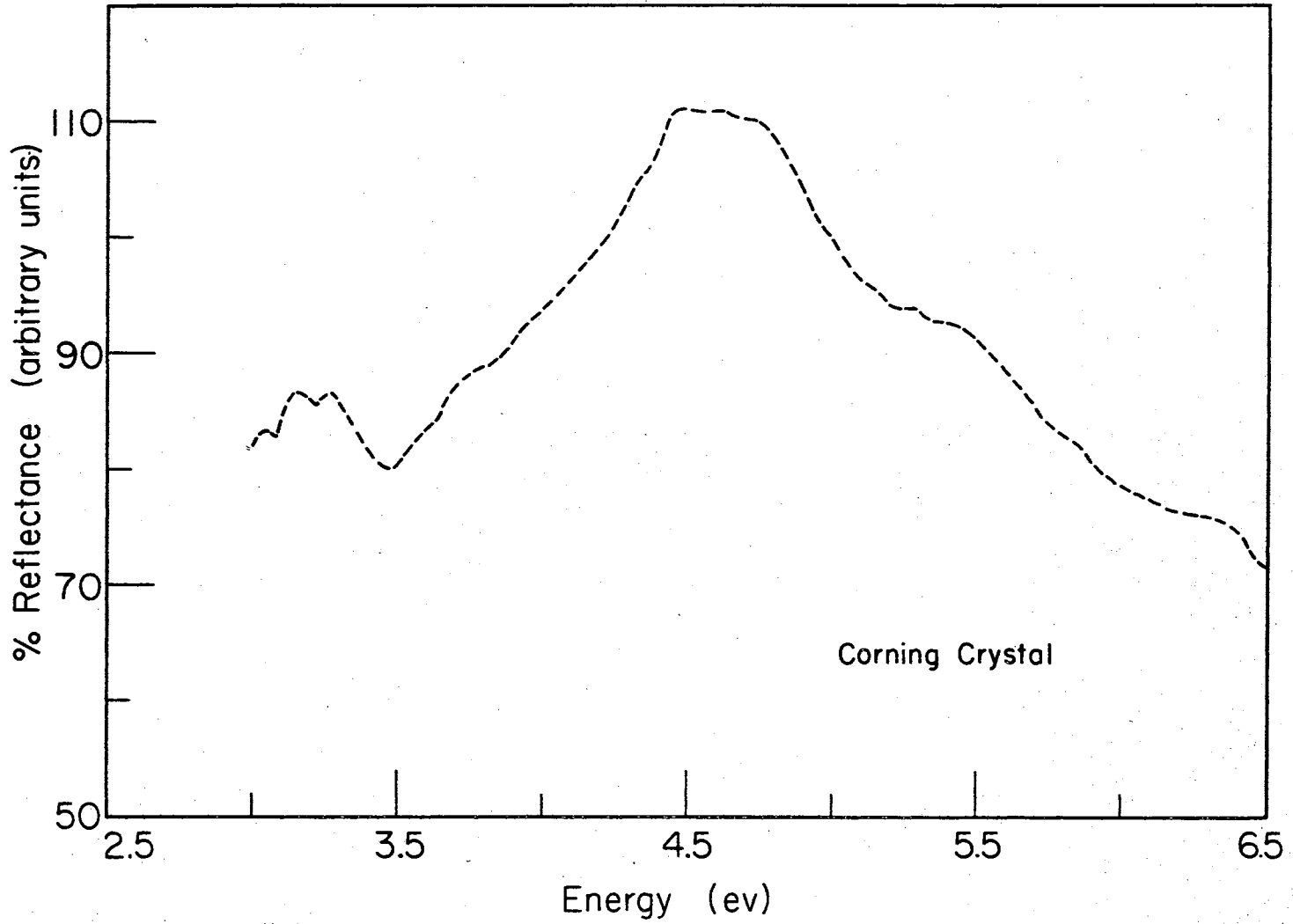


Figure 8. Reflectance vs Energy for a Vapor-Grown Stannic Oxide Single Crystal

vs energy structure. However, the curve obtained for the natural sample of stannic oxide agrees quite well in shape with that obtained for the E/c data of rutile as given by Cardona and Harbeke (37). Apparently the oxides in the space group D_{4h}^{14} behave as do the metals and intermetallics in that the shape of the reflectance curve appears to be a function of the structure of the system rather than a function of the type of ion within the system being studied. This agrees with various theoretical proposals which have been advanced (10,34,47). However, there is not enough data currently available for the members of this particular space group to state that such is always the case. If it were, the shape of the E/c curve given by Cardona and Harbeke for rutile could be used to extract a similar stannic oxide curve.

Thus, one must keep in mind that there is indeed a difference between the two spectra obtained and that this is a real and necessary difference arising from the difference in polarization of the light incident upon the samples with respect to their c-axis orientations. From these curves, it should be possible to determine some of the energy differences for allowed optical transitions by correlation of the proper selection rules with the band structure calculation.

CHAPTER IV

GENERAL BAND THEORY FORMALISM

Every theoretical treatment of a physical system has as its ultimate goal the establishment of a model from which the properties of the system under study may be extracted. When dealing with a system which displays many different chemical and physical characteristics, it is not uncommon to have almost as many different models as there are research efforts. Thus, for example, the treatment of some of the gross optical and electrical properties of a solid may be handled very nicely using a flat band model; however, if all such properties are to be treated simultaneously, this model proves to be of limited value. In general, the establishment of a good model requires that some details of the actual order of magnitude of the forces which act on the microscopic level be known. Indeed, if all such forces were fully tabulated and categorized for any solid, it might be possible to build a mathematical model of the system which would predict exactly its gross physical and chemical properties. However, at the present time, so little is definitely known about the forces acting on an electron as it traverses a lattice that such complete models for solids are not yet in sight. For this reason, the general approach for obtaining information pertaining to the allowed electron energy bands of solids and the ultimate application of this information to give order-of-magnitude estimates and mathematical forms for the forces acting on an electron in a periodic poten-

tial has led to band structures that are seldom in agreement with experiment. The reason for the lack of agreement between theory and experiment (usually of an order of 25%) lies in an inaccurate determination of the mathematical form of the potential seen by the electron. As a result, several techniques for handling such problems have been proposed and exploited. Regardless of the approach, however, the plan of calculation ultimately revolves about some self-consistent effort wherein given a potential which predicts a few of the measureable properties of the system, the next step involves performing a calculation which is then used for checking the effectiveness of the chosen potential to predict another measureable property. Generally, the potential does not predict the property to the desired accuracy. As a result, the potential is modified anew until this new property is predicted. After such modification as is necessary, the prediction of a different effect is attempted and unless this effect is correctly predicted by the model, the potential is modified again. In this manner one attempts to build a mathematical model of the system that predicts as many of its properties as are measureable and predictable within the framework of the theory being used. After ascertaining the final mathematical form of the potential which best satisfies the situation, some insight as to the overall force which acts upon an electron as it moves through the lattice may be extracted. This is the ultimate goal of any such calculation.

As may be inferred from the above introduction, such calculations are not easily obtained unless a great deal is known about the physical system under study. Thus, the problem at first glance seems intractable. However, using the one electron theory of solids along with the available computer methods of calculation, some rudimentary ideas as to the

form and symmetries of the bands for any solid may be obtained.

Many different methods of calculation have been proposed by various workers. However, the details of calculation are usually of a complexity sufficient to be omitted in a general exposition. As an example of the many different types of calculational approaches the reader is referred to the following references in which the various methods are treated in some detail (48,49,50,51,52,53).

Although space will not allow an exposition of the details of all of the different types of calculation currently being used, it is felt that the method of orthogonalized plane waves should be given a brief review at this point as it leads quite naturally into the method of pseudopotentials and thus lends particular insight into the motivation for choosing a pseudopotential formalism for the calculation pertaining to stannic oxide.

The method of orthogonalized plane waves (OPW) shall be treated following Herman (52), Callaway (48), and Jones (51). This method consists of expanding the core wave functions in terms of linear combinations of atomic orbitals. Further, the non-core wavefunctions are expanded in terms of plane waves each of which has been orthogonalized to the core functions by the Schmidt process. The orthogonalization process serves to introduce into the wavefunction a nodal structure which approximates the actual one quite closely. This leaves a slowly varying portion to be represented by plane waves. One may thus expect a relatively small number of OPW's to be necessary to describe the wavefunctions for valence and low-lying conduction bands. Although convergence is rather slow for the electron states that are above the lowest valence band state, it is sufficient to make the method practical.

Although the approach requires no special assumptions to be made about the crystal potential except that it have the proper symmetry, there are inherent difficulties with the method which shall be mentioned later. It is now assumed for the sake of simplicity that the crystal system dealt with contains only one type of atom. Following the description given by Jones (51), let $\chi_{\underline{k}\underline{n}}(\underline{r})$ denote a Bloch wavefunction for one of the electronic states belonging to the core and let

$$\psi_{\underline{k}\underline{i}} = e^{i(\underline{k} + \underline{l}_i B) \cdot \underline{r}} \sum_n \mu_{in} \chi_{\underline{k}\underline{n}} \quad (1)$$

The summation is over all electronic states in the core, i.e., over all states whose energies are less than the energy of the lowest state in the valence band of the crystal. The core wavefunctions form an orthogonal set and it will be assumed that they are normalized so that

$$\int_{\text{all space}} \chi_{\underline{k}\underline{n}}^* \chi_{\underline{k}\underline{m}} d^3r = \delta_{nm} \quad (2)$$

The condition which determines the μ_{in} is

$$\int_{\text{all space}} \chi_{\underline{k}\underline{n}}^* \psi_{\underline{k}\underline{i}} d^3r = 0 \quad (3)$$

or

$$\mu_{in} = \int_{\text{all Space}} e^{i(\underline{k} + \underline{l}_i B) \cdot \underline{r}} \chi_{\underline{k}\underline{n}}^*(\underline{r}) d^3r \quad (4)$$

From the definition of \underline{l}_B it will be observed that for every \underline{k} there is

a complete set of functions $\psi_{\underline{k}i}$, each member of the set being associated with a reciprocal lattice point \underline{lB} . The required wavefunction in the valence band, with wavevector \underline{k} can be expressed as

$$\Psi_{\underline{k}}(\underline{r}) = \sum_i \beta_i \psi_{\underline{k}i}(\underline{r}). \quad (5)$$

A very satisfactory feature of the method now becomes evident. Since all $\psi_{\underline{k}i}$ are orthogonal to the core states, it follows by the variation process that if Ψ is regarded as a variation function, the energy of this state converges to the correct value as the number of terms in the summation is increased.

Before applying the variational principle, it should be noted that the $\psi_{\underline{k}i}$ for different i are not orthogonal to one another. Thus, by making use of the definition of $\psi_{\underline{k}i}$ and the definition of \mathcal{M}_{in} ,

$$\int_{\text{ALL SPACE}} \psi_{\underline{k}j}^* \psi_{\underline{k}i} d^3r = -\sum_n \mathcal{M}_{jn}^* \mathcal{M}_{in}. \quad (6)$$

If $V(\underline{r})$ denotes the potential energy of any electron in the crystal and the Hamiltonian has the form:

$$H = -\frac{\hbar^2}{2m} \nabla^2 + V(\underline{r}) \quad (7)$$

the variation principle requires

$$\int_{\text{ALL SPACE}} \Psi_{\underline{k}}^* (H - E) \Psi_{\underline{k}} d^3r = 0 \quad (8)$$

which in turn requires

$$\det |H_{ij} - E A_{ij}| = 0 \quad (9)$$

The degree of this equation for E is determined by the number of variation parameters β_i included when defining Ψ . The usefulness of the method is largely due to the fact that good results can often be obtained with a small number of OPW's when dealing with a metal.

The matrix elements H_{ij} are defined by $\langle \psi_{kj} | H | \psi_{ki} \rangle$ which simplifies after multiplying out the factors. For example

$$H \chi_{kn} = E_{kn} \chi_{kn} \text{ may be used.} \quad (10)$$

The usual practice is to express the χ_{kn} functions by the LCAO approximation as follows:

$$\chi_{kn} = \sum_n e^{ik \cdot \underline{A}n} \phi_n(\underline{r} - \underline{A}n) \quad (11)$$

where the radial part of the orbital ϕ_n is obtained as a numerically tabulated function.

This method is not without several troublesome features of which two shall be mentioned. At first sight it might be supposed that it would be possible to use existing Hartree functions for the core orbitals ϕ_n . This is not the case, however, since it is essential that we use orthogonal functions so that

$$\langle \phi_m(\underline{r}) | \phi_n(\underline{r}) \rangle = 0 \quad (12)$$

if full advantage of the method is to be taken. H_{ij} contains terms of the form $\langle \phi_m | H | \phi_n \rangle$ which vanish if the functions are orthogonal. Hartree functions do not form an orthogonal set because different orbitals are determined by different Hamiltonians in the Hartree method. If such non-orthogonal functions are used, the integral $\langle \phi_m | H | \phi_n \rangle \neq 0$ and is far from being negligible in most cases. Thus, a great many terms in the variational function would have to be used to obtain satisfactory results.

The second difficulty arises when solutions are required at symmetry points of the Brillouin zone. In practice, most calculations are made at such points. At these points, the wavefunctions have specified symmetries and hence in place of the exponential in defining Ψ , a symmetrized plane wave occurs. This causes a corresponding change in integrand for μ_{in} and hence solely from the symmetry of the factor multiplying χ_{kn}^* many of the μ_{in} vanish identically. This implies that many terms must be used in the sum for Ψ . Therefore, in practice (at these points) the coefficients μ are chosen rather than calculated and are selected in such a way as to give the ψ_{ki} a form near the nuclei which is rather like that anticipated for the crystal wavefunction. Due to this arbitrariness in the choice of trial functions, the reliability of the method then rests on the convergence of the variational procedure. Confidence in the result thus depends on showing that as the number of terms defining Ψ increases, the eigenvalues converge to a well-defined limit.

When these difficulties are coupled with the fact that the previous formalism was given for a monatomic lattice with only one valence

electron, it may be seen readily that the insertion of another atomic species as well as the taking into consideration of all valence electrons from both types of atoms would lead to a problem whose solution would be extremely difficult.

As a result of the many difficulties encountered when using this method another approach which contains the merits of the past treatment yet avoids its more serious faults might be desired. Such an approach became available when Phillips and Kleinman (55) noted that the effect of the orthogonalization terms was to cancel part of the attractive potential. This cancellation arose through the difference in sign between the orthogonalization terms and the attractive potential. Although Phillips (54) was the first to investigate and utilize this cancellation to the utmost, it is interesting to note that the sum of attractive and repulsive potentials so generated leads to a treatment of the electron in the lattice in terms of what is essentially a nearly-free-electron approach. This idea (NFE) was advanced by Jones in his text (51) at about the same time as being the only approach which has any real correlation with experiment.

The method now being considered is that of the pseudopotential. Since the earliest work regarding the treatment of electrons in a lattice by this means (55), many other papers have been published which utilize this cancellation and attempt to use the resulting weak potential to calculate the bands for metals. Many different pseudopotentials have been postulated for different cases but they have generally all been shown to be equivalent mathematically (59). For the sake of reference the reader is referred to the text by Harrison (49) and the papers (56,57,58,59,60,61,62,63,64,65,66,67,68,69).

Following Phillips and Kleinman (55) the first assumption is that all electrons move in the same potential. This assumption leads to what is known as the "local" pseudopotential and shall be explained when the limitations and overall character of the pseudopotential formalism are stated. At first only valence and conduction band wave functions having s or p atomic character at the center of the zone are considered. These restrictions may be removed later. Imagine that the exact crystal wavefunction ψ_{α} which has s or p atomic symmetry and transforms according to an irreducible representation Γ of the point group is known. Since ψ_{α} must be orthogonal to the core states of similar symmetry,

$$\psi_{\alpha} = \phi_{\alpha} + \sum_n a_{\alpha}^n \phi_{\alpha}^n \quad \text{where} \quad (13)$$

$$a_{\alpha}^n = - \langle \phi_{\alpha} | \phi_{\alpha}^n \rangle \quad (14)$$

Had ϕ been chosen to be a single plane wave, Herring's OPW results would follow. However, equations (13) and (14) already show a trivial mathematical but physically important, simplification, in that valence wavefunctions of a given symmetry type need be orthogonalized only to that symmetry type core function.

ϕ_{α} is defined to be the "smooth" part of ψ_{α} . Thus, since

$$H \psi_{\alpha} = E \psi_{\alpha}, \quad (15)$$

substitution of (13) into (15) results in

$$H \phi_{\alpha} + \sum_n a_{\alpha}^n (E^n - E) \phi_{\alpha}^n = E \phi_{\alpha} \quad (16)$$

where $H \psi_n = E_n \psi_n$. Now introduce $V_r = \sum_n a_n (E_n - E) \psi_n / \psi$ and (16) assumes the desired form

$$(H + V_r) \psi = E \psi. \quad (17)$$

If H is broken into its kinetic and potential energy operators the potentials may be grouped together to define a new potential energy, the pseudopotential.

Although such a derivation appears to be quite simple, one must recall the several simplifying assumptions that have been made. The results obtained are often only approximately correct even at the center of the Brillouin zone due to the mixing of the s and p -like character atomic states when defining the repulsive potential. For a complete treatment of this subject, the reader is referred to reference (55).

There are three fundamental physical approximations which enter the theory and must be stated for the sake of completeness. The reader is referred to Harrison (49) for a more general treatment of these ideas. The first approximation is the "self-consistent-field" approximation. This simply means that one replaces the interaction between electrons by a potential which is to represent some average interaction. This potential depends upon the states which are occupied by electrons, and these states, in turn, depend upon the potential; thus the potential must be computed self-consistently. Ultimately, the only important interaction between electrons is the coulomb repulsion, but this can be conveniently divided into three distinct contributions. The first is the Hartree potential, obtained by computing the time average of the electron distribution and then using Poisson's equation to determine

the corresponding potential. The second is the correction for the potential seen by an electron due to the Pauli principle; i.e., if an electron of the same spin can lie at that point, simply because of the anti-symmetric nature of the wavefunctions. This effectively gives a hole in the electron distribution and gives rise to the exchange interaction. Into the third contribution are lumped the remaining corrections which arise from the correlation motion of the electrons: this is the correlation energy.

The second fundamental approximation is the separation of electron energy levels into core states and conduction-band states and the treatment of the core states as localized and small. This "small core approximation" is used in three distinct ways. Assuming that adjacent cores do not overlap, there is no direct interaction between ions except their coulomb repulsion. Secondly, the variation over the core of potentials due to the conduction electrons and adjacent ions is neglected. It follows then that the core wavefunctions are the same as in the isolated ion, although their energies differ from those of the isolated ion. Finally, in the integration of products of various smooth functions and core wave functions, the variation of the smooth functions over the ion is neglected, allowing them to be evaluated at the nucleus and taken out of the integral. This approximation is very good for the alkali and polyvalent metals.

The third fundamental approximation is the assumption that it is proper to use perturbation theory in computing the conduction band states.

Although the applicability of each of these approximations must be thoroughly investigated and estimated in a "good" pseudopotential cal-

ulation, many of the aforementioned effects have been neglected in the present stannic oxide calculation in favor of utilizing an empirical pseudopotential technique wherein these effects are omitted in the first approximation for everything other than the calculation of the atomic form factors (the Fourier transforms of the assumed pseudopotentials). With this in mind, the first calculation made is not expected to give results which agree with all of the data on hand but can be used as a starting point for a later attempt to predict some of the gross physical properties of the system in agreement with the self-consistent type of calculation mentioned in the introduction.

CHAPTER V

THE CALCULATION

The approximation being used requires that the form factors of the two atomic species be known. Since Weisz (70) has given the form factor of white tin which also has a tetragonal structure, his data were used as a starting point for this calculation. These data were supplemented by those of Harrison (49) in order that a better curve for the tin form factor could be drawn. However, the data extracted in this manner were not sufficient for this calculation due to the different unit cell volumes of white tin and stannic oxide. Since the form factor is defined to be the Fourier transform of the assumed pseudopotential, it may be seen that for a first approximation the adjustment necessary in attempting to utilize these data for the stannic oxide calculation involves a simple ratio of the unit cell volumes of white tin and stannic oxide.

The Fourier transform of the pseudopotential would normally be found by integration as:

$$v(|\underline{k}|) = \frac{N}{\mathcal{V}} \int_{\mathcal{V}} e^{i\underline{k} \cdot \underline{r}} v(\underline{r}) d^3 \underline{r} \quad (1)$$

where \mathcal{V} is the unit cell volume and N is the number of atoms per unit cell. At this point a simplification is to be made in that the domain of integration will be taken to extend over all of space rather than over the unit cell of the crystal which is by definition the unit

of periodicity for the system under study. This approach appears valid since the repulsive part of the potential is usually of a rather limited range due to the finite extension of the core wavefunctions throughout space.

Since there are two tin atoms per unit cell in both white tin and stannic oxide, it is possible to write:

$$v_1(|\underline{k}|) = \frac{2}{\Omega_1} \int_{\text{ALL SPACE}} e^{i\underline{k} \cdot \underline{r}} v_1(\underline{r}) d^3\underline{r} \quad (\text{white tin}) \quad (2)$$

$$v_2(|\underline{k}|) = \frac{2}{\Omega_2} \int_{\text{ALL SPACE}} e^{i\underline{k} \cdot \underline{r}} v_2(\underline{r}) d^3\underline{r} \quad (\text{stannic oxide}). \quad (3)$$

The next assumption is that the spatially dependent potential for tin in the two different environments is not appreciably different so that the two integrands are the same. If this be the case,

$$\frac{v_1(|\underline{k}|)}{v_2(|\underline{k}|)} = \frac{\Omega_2}{\Omega_1}. \quad (4)$$

Thus, with very crude assumptions, it is possible for an initial potential form factor for the tin atom in stannic oxide to be extracted from that given for white tin.

The oxygen form factor may also be acquired by attempting a similar modification of the form factor given for oxygen in the magnesium oxide lattice (71). However, when the present calculation was initiated, these results were not available. Therefore, an attempt was made to calculate a form factor for oxygen following Kleinman and Phillips (55).

Such a calculation requires that a few approximations be made pertaining to the repulsive part of the pseudopotential since a priori, the electron wavefunction in the crystal is not known.

The repulsive part of the pseudopotential was therefore calculated using (in terms of its Fourier transform)

$$V_{\mathbf{r}}^1(\mathbf{k}) = (E - E_{1s}) \frac{N}{\Omega} \int_{\text{All Space}} \left\{ \int_{\text{All Space}} \psi_{1s}(\mathbf{r}) d^3r \right\} \psi_{1s}(\mathbf{r}) e^{i\mathbf{k}\cdot\mathbf{r}} d^3r. \quad (5)$$

The net form factor was then found by the addition of the Fourier transform of the self-consistent potential given by Herman and Skillman (72).

In the above calculation the following parameters were used:

TABLE I
OXYGEN FORM FACTOR PARAMETERS

E(Rydbergs)	E_{1s} (Rydbergs)	N	Unit Cell Volume
3.5	-39.456	6	475.289 (Atomic Units)

The approach given above is not sufficient in itself because it neglects an additional repulsive term which arises due to the valence electrons. This additional term could be calculated from first principles if the valence band and conduction band wavefunctions were known. However, since this is not the case, it is required that the position of the resultant oxygen form factor be adjusted until there is (in the overall calculation) some degree of continuity between compatible electron states in the crystal. Figures 9 and 10 indicate the initial form factors used while Figure 11 contains the final shape and relative positioning of the two form factors as used. It should be mentioned at this point that the final oxygen form factor agrees quite nicely with that obtained for oxygen in magnesium oxide (71) although the oxygen form factor in this latter case is shifted somewhat with respect to the data given in Figure 11.

After acquiring the initial form factors, the calculation of electron energy bands proceeded by considering a secular equation containing fifty-five plane waves. This secular equation was factored using standard group theoretical techniques which shall be illustrated via example. The results of the factorization can be compared with Herman's (73) results for the diamond structure to indicate differences in mathematical form for factored secular equations which are related to different space groups. However, before the various matrix elements are calculated, and the secular equation factored, it is necessary that a word be said about the notation which will be used in the following treatment of the problem.

The Hamiltonian operator may be written in standard form

$$H_{op} = \frac{p^2}{2m} + V(r). \quad (6)$$

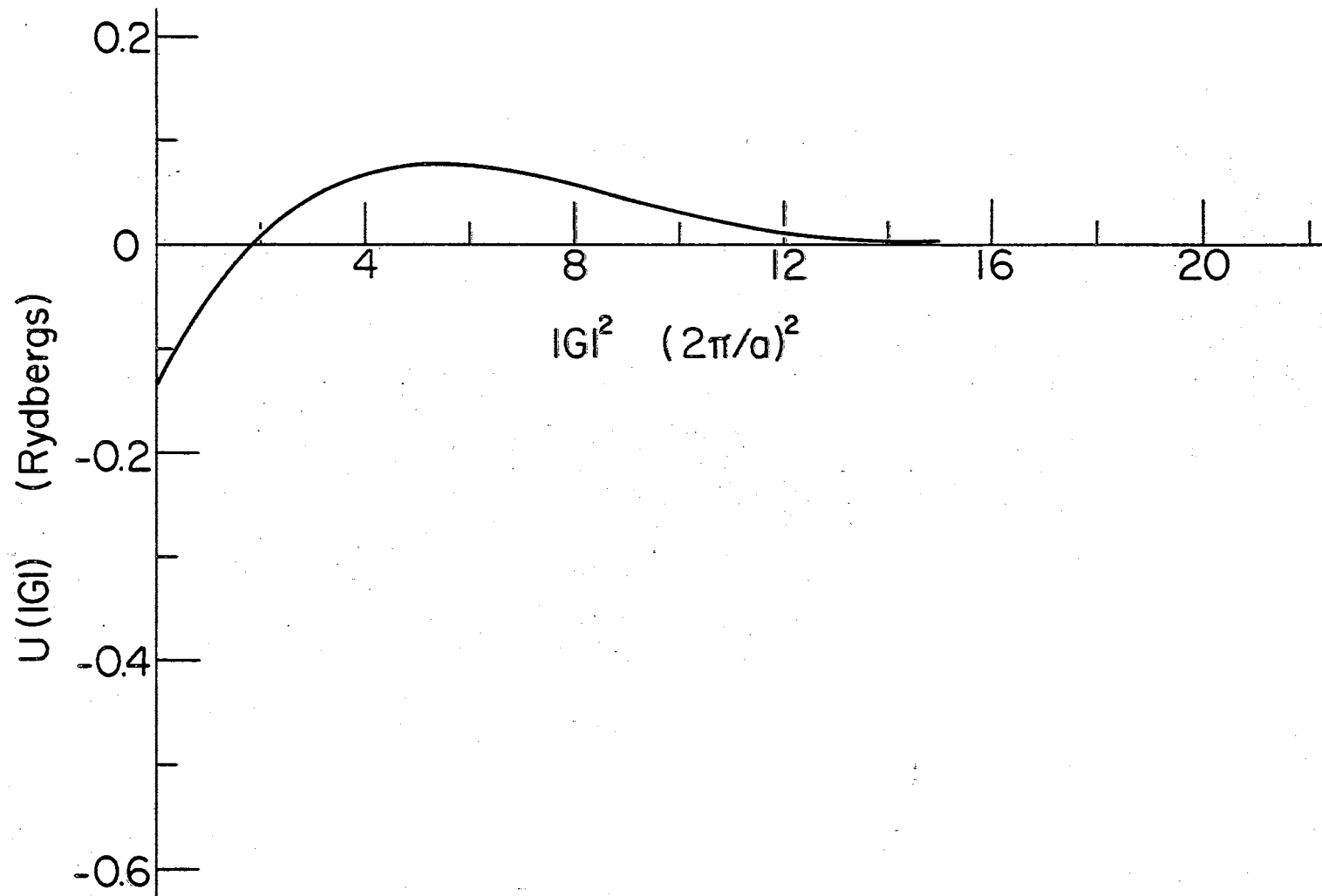


Figure 9. Initial Oxygen Form Factor

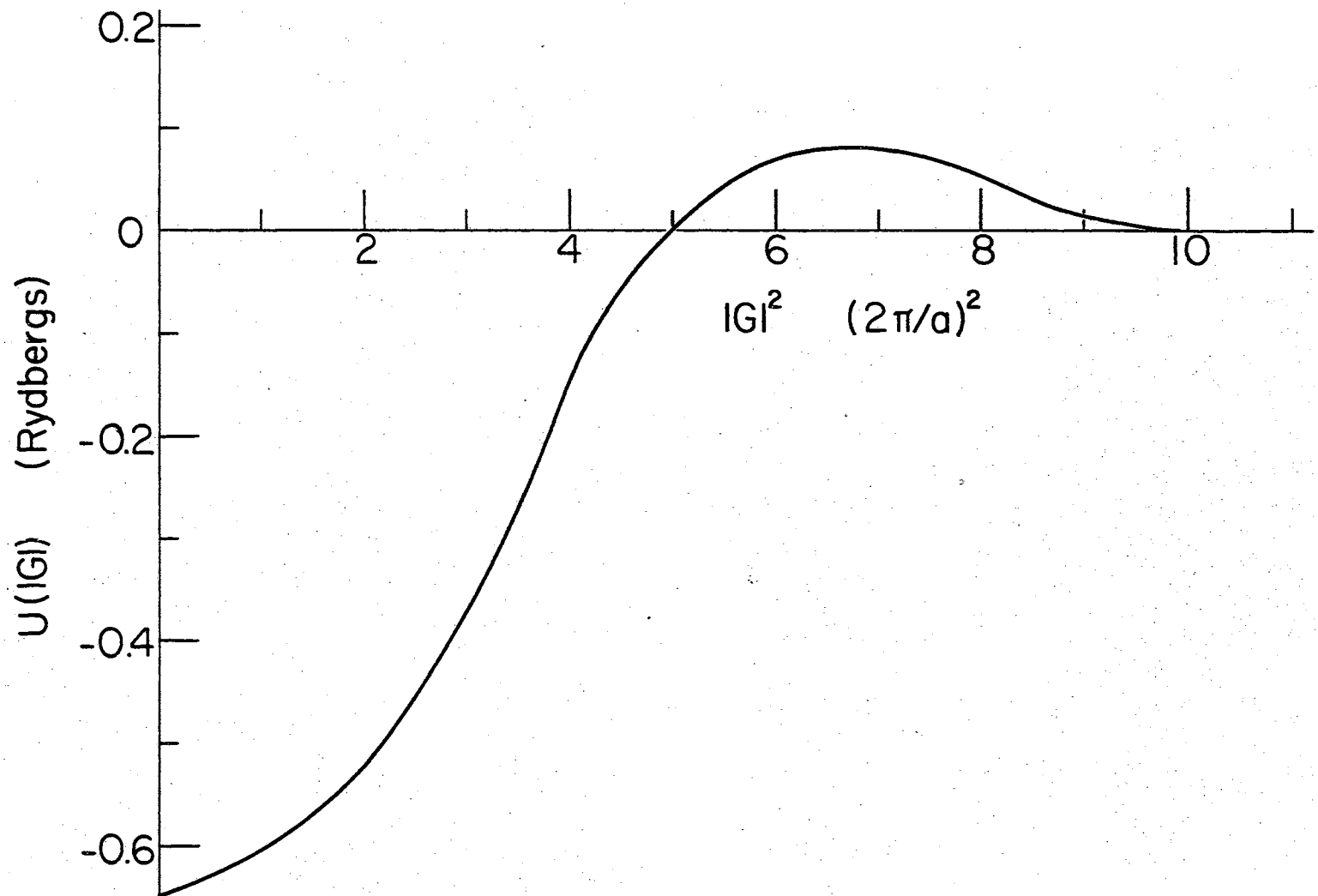


Figure 10. Initial Tin Form Factor

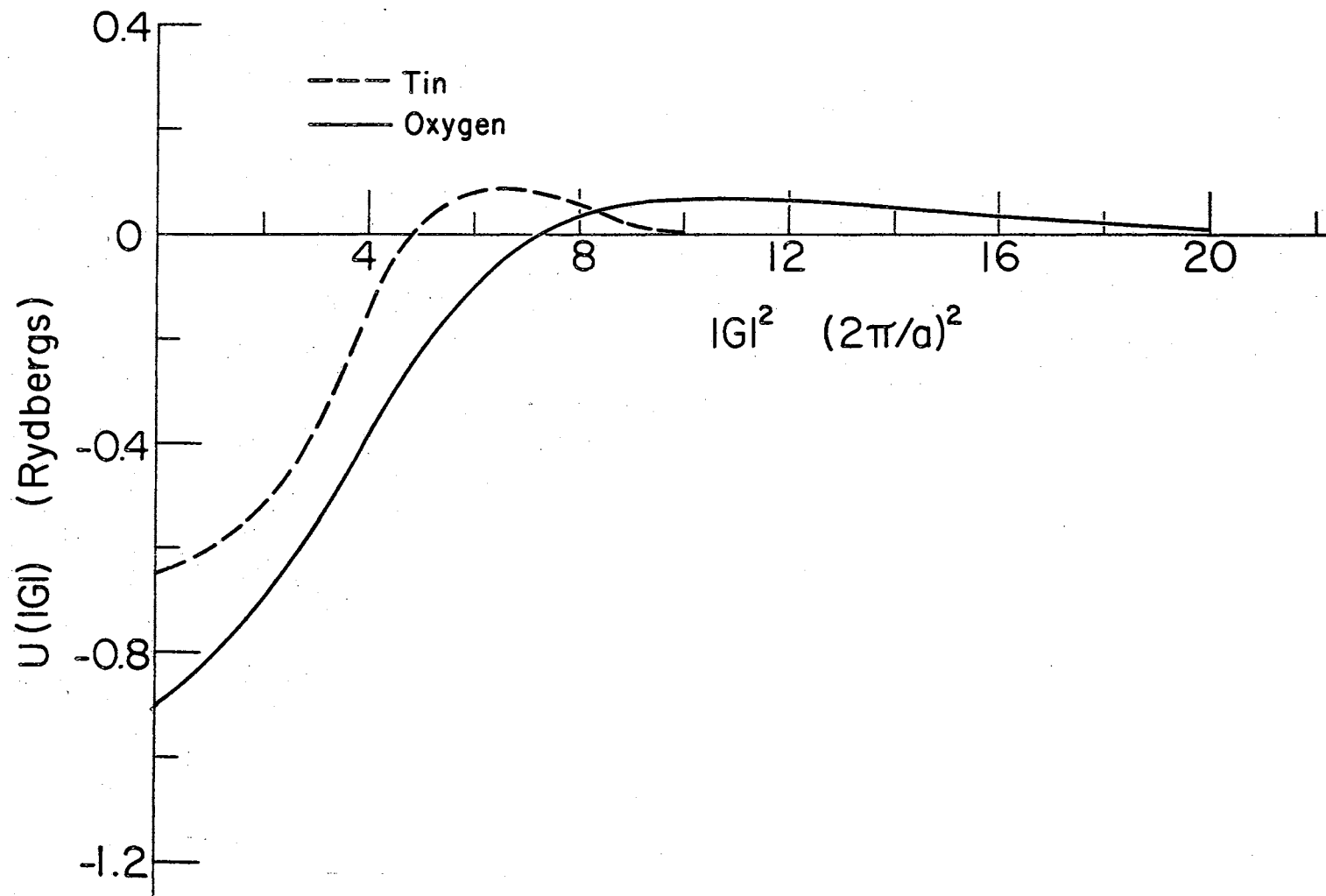


Figure 11. Final Tin and Oxygen Form Factors Used in the Calculation

Using the usual techniques of associating an operator with an observable,

$$p \rightarrow \frac{\hbar}{i} \frac{\partial}{\partial q} \quad (7)$$

$$q \rightarrow q.$$

If normalized Bloch functions are used as a basis and \underline{k} and \underline{k}' differ by no more than a reciprocal lattice vector, the expectation value of the energy may be found quite simply by

$$\langle \underline{k} | H_{op} | \underline{k}' \rangle = \langle \underline{k} | \frac{p^2}{2m} | \underline{k}' \rangle + \langle \underline{k} | V(\underline{r}) | \underline{k}' \rangle \quad (8)$$

where

$$| \underline{k} \rangle = \psi_{\underline{k}}(\underline{r}) = e^{i\underline{k} \cdot \underline{r}} U(\underline{r}) \quad (9)$$

and $U(\underline{r})$ has the same periodicity as the lattice. If the \underline{k} represent plane waves, the result may be seen to have the form

$$H = \frac{\hbar^2(\underline{k} - lB)^2}{2m} + \langle \underline{k} | V(\underline{r}) | \underline{k}' \rangle. \quad (10)$$

Utilization of the diffraction model (3) band theory formalism makes the acquisition of matrix elements relatively simple. This technique shall also be illustrated by example later in this section.

If it were impossible to use any symmetry arguments, an N by N secular equation could be solved which would yield both energies and eigenvectors along any axis of the first Brillouin zone. However, the results would be of questionable value since little could be said pertaining to the symmetry of the resultant eigenstates and thus the identification of possible electron transitions in stannic oxide would be

hindered because the initial and final state symmetries would remain unknown.

Therefore, the symmetry of the system shall be built into the calculation by factoring the N by N secular equation. The resultant secular equation may be written in block diagonal form wherein each block has a particular symmetry associated with it. This process shall now be illustrated by using the $(1,1,1)$ set of wavevectors and compared with Herman's work (73) on the diamond structure.

At the center of the zone, the free-electron energy is given by

$$E = l_1^2 + l_2^2 + l_3^2 (a/c)^2 = 4.23 \quad (11)$$

Table II contains the D_{4h} character system while Table III contains all of the elements of this system with the substitution appropriate for the D_{4h}^{14} space group. In this analysis the body centered atom of the unit cell is considered to be located at the origin of coordinates; thus, the positions of the tin and oxygen atoms are those given by Wyckoff (74) and yield the following structure factor:

Tin	Oxygen
$1 + \exp[i(l_1 + l_2 + l_3)]$	$2 \cos 2\pi u (l_1 + l_2) +$ $2 \exp\{i\pi(l_1 + l_2 + l_3)\} \cos 2\pi u (l_1 - l_2)$

The wavefunctions that are accidentally degenerate at this energy in the free electron approximation may be written as follows:

$$\begin{aligned} a &= (1,1,1) & e &= (1,\bar{1},\bar{1}) \\ b &= (1,1,\bar{1}) & f &= (\bar{1},1,\bar{1}) \end{aligned}$$

TABLE II
 D_{14} CHARACTER SYSTEM

Representation	\underline{C}_1	\underline{C}_2	\underline{C}_3	\underline{C}_4	\underline{C}_5	\underline{C}_6	\underline{C}_7	\underline{C}_8	\underline{C}_9	\underline{C}_{10}	Substitution
1	1	1	1	1	1	1	1	1	1	1	$1 + \frac{1}{2}(x^2 + y^2) - z^2$
2	1	1	1	-1	-1	1	1	1	-1	-1	$xy(x^2 - y^2)$
3	1	1	-1	1	-1	1	1	-1	1	-1	$x^2 - y^2$
4	1	1	-1	-1	1	1	1	-1	-1	1	xy
5	2	-2	0	0	0	2	-2	0	0	0	(yz, zx)
1	1	1	1	1	1	-1	-1	-1	-1	-1	$xyz(x^2 - y^2)$
2	1	1	1	-1	-1	-1	-1	-1	1	1	z
3	1	1	-1	1	-1	-1	-1	1	-1	1	xyz
4	1	1	-1	-1	1	-1	-1	1	1	-1	$z(x^2 - y^2)$
5	2	-2	0	0	0	-2	2	0	0	0	(x, y)
	E	C_2	TC_1^+	TR_1^+	R_1^+	J	M_3	TJC_1^+	T_{m1}^+	m_1^+	
			TC_1^{-1}	TR_2	R_2'			TJC_1^{-1}	T_{m2}	m_2'	

TABLE III
 SUBSTITUTIONS FOR D_{14}^{4h}

Element	Substitution	No.	Element	Substitution	No.
E	xyz	1	J	xyz	9
C_2	xyz	2	m_3	xyz	10
TC_1	y+a/2, x+a/2, z+c/2	3	TJC_1	y+a/2, x+a/2, z+c/2	11
TC_1^{-1}	y+a/2, x+a/2, z+c/2	4	TJC_2^{-1}	y+a/2, x+a/2, z+c/2	12
TR_1	x+a/2, y+a/2, z+c/2	5	Tm_2	x+a/2, y+a/2, z+c/2	13
TR_2	x+a/2, y+a/2, z+c/2	6	Tm_1	x+a/2, y+a/2, z+c/2	14
R_1'	yxz	7	m_1'	y,x,z	15
R_2'	yxz	8	m_2'	yxz	16

About this notation: Have herein used the D_{4h}^{14} point group notation and this may be correlated with past notation by:

$E = E$	$TC_1 = Tmm_2$	$J = J$	$TJC_1 = TmR_1$
$C_2 = C$	$TC_1^{-1} = Tmm_1$	$m_3 = m_3$	$TJC_1^{-1} = TmR_2$
$TR_1 = Tmm_3$	$R_1' = R_1$	$Tm_1 = Tm$	$m_1' = m_1$
$TR_2 = TmJ$	$R_2' = R_2$	$Tm_2 = TmC_2$	$m_2' = m_2$

$$\begin{aligned} c &= (\overline{1}, \overline{1}, 1) & g &= (\overline{1}, \overline{1}, 1) \\ d &= (\overline{1}, 1, 1) & h &= (\overline{1}, \overline{1}, \overline{1}) \end{aligned}$$

Each triple corresponds to a wavefunction obtained by substituting its components into the general wavefunction at the center of the zone which has the following standard form

$$\psi_{\Gamma} = e^{-2\pi i \left\{ \frac{l_1 x}{a} + \frac{l_2 y}{a} + \frac{l_3 z}{c} \right\}}. \quad (12)$$

The space group under consideration contains a diagonal glide which unlike the threefold glide of the diamond structure, is twofold in nature in that it has glide planes which are perpendicular to the faces of the unit cell of area ac and located in the geometric center of the faces, i.e. they bisect the faces mentioned. As a result of the existence of this diagonal glide, there is in the space group an inherent nonprimitive translation that must be considered. Application of this translation operation to the general wavefunction at this point yields

$$T(a/2, a/2, c/2) \psi_{\Gamma} = e^{-2\pi i \left\{ \frac{l_1(x + c/2)}{a} + \right.} \quad (13)$$

$$\left. \frac{l_2(y + a/2)}{a} + \frac{l_3(z + c/2)}{c} \right\}} = e^{-\pi i \frac{l_1 l_2}{2}} \psi_{\Gamma}$$

Thus, the effect of the translation operation is to pre-multiply the wavefunction by ± 1 .

Table IV contains the effect of application of the sixteen operations to the functions previously listed as triples.

Using standard procedures, the reducible representation and its irreducible representation sum is given for stannic oxide as

TABLE IV
APPLICATION OF SPACE GROUP OPERATIONS TO (1,1,1) WAVEFUNCTIONS

Operation	Wavefunction								R
	a	b	c	d	e	f	g	h	
1	a	b	c	d	e	f	g	h	8
2	g	h	d	c	f	e	a	b	0
3	-c	-e	-g	-a	-h	-b	-d	-f	0
4	-d	-f	-a	-g	-b	-h	-c	-e	0
5	-f	-d	-h	-b	-g	-a	-e	-c	0
6	-e	-c	-b	-h	-a	-g	-f	-d	0
7	h	g	e	f	c	d	b	a	0
8	b	a	f	e	d	c	h	g	0
9	h	g	f	e	d	c	b	a	0
10	b	a	e	f	c	d	h	g	0
11	-f	-d	-b	-h	-a	-g	-e	-c	0
12	-e	-c	-h	-b	-g	-h	-d	-f	0
13	-c	-e	-a	-g	-b	-h	-a	-f	0
14	-d	-f	-g	-a	-h	-b	-c	-e	0
15	g	h	c	d	e	f	a	b	4
16	a	b	d	c	f	d	g	h	4

8/2 = 4

$$\Gamma_{R}\{(1,1,1)\} = \Gamma_1 + \Gamma_4 + \Gamma_5 + \Gamma_{2'} + \Gamma_{3'} + \Gamma_{5'} \quad (14)$$

while for diamond one has

$$\Gamma_{R}\{(1,1,1)\} = \Gamma_1 + \Gamma_{2'} + \Gamma_{25'} + \Gamma_{15} \quad (\text{Cubic System}). \quad (15)$$

The next step in the calculation involves using this result to extract symmetrized combinations of plane waves that may be used in later calculations. The procedure is standard but shall be stated for the sake of completeness. The most symmetric or Γ_1 representation has only positive characters. However, the translation changes the sign of the wavefunction since the sum $l_1 + l_2 + l_3$ is odd. As a result, the wavefunction of this symmetry has both positive and negative parts. Table V contains the six irreducible representations and their corresponding wavefunctions, while Table VI contains the same result for the cubic system as derived by Herman.

In a similar fashion, other sets of triples may be considered. The first nineteen of these are given in Table VII. These are now to be used to illustrate the factorization of the secular equation.

Using only the eight triples in the degenerate (1,1,1) state, the secular equation is transformed into that shown in Figure 12. This result should be compared with that of Herman which is shown in Figure 13.

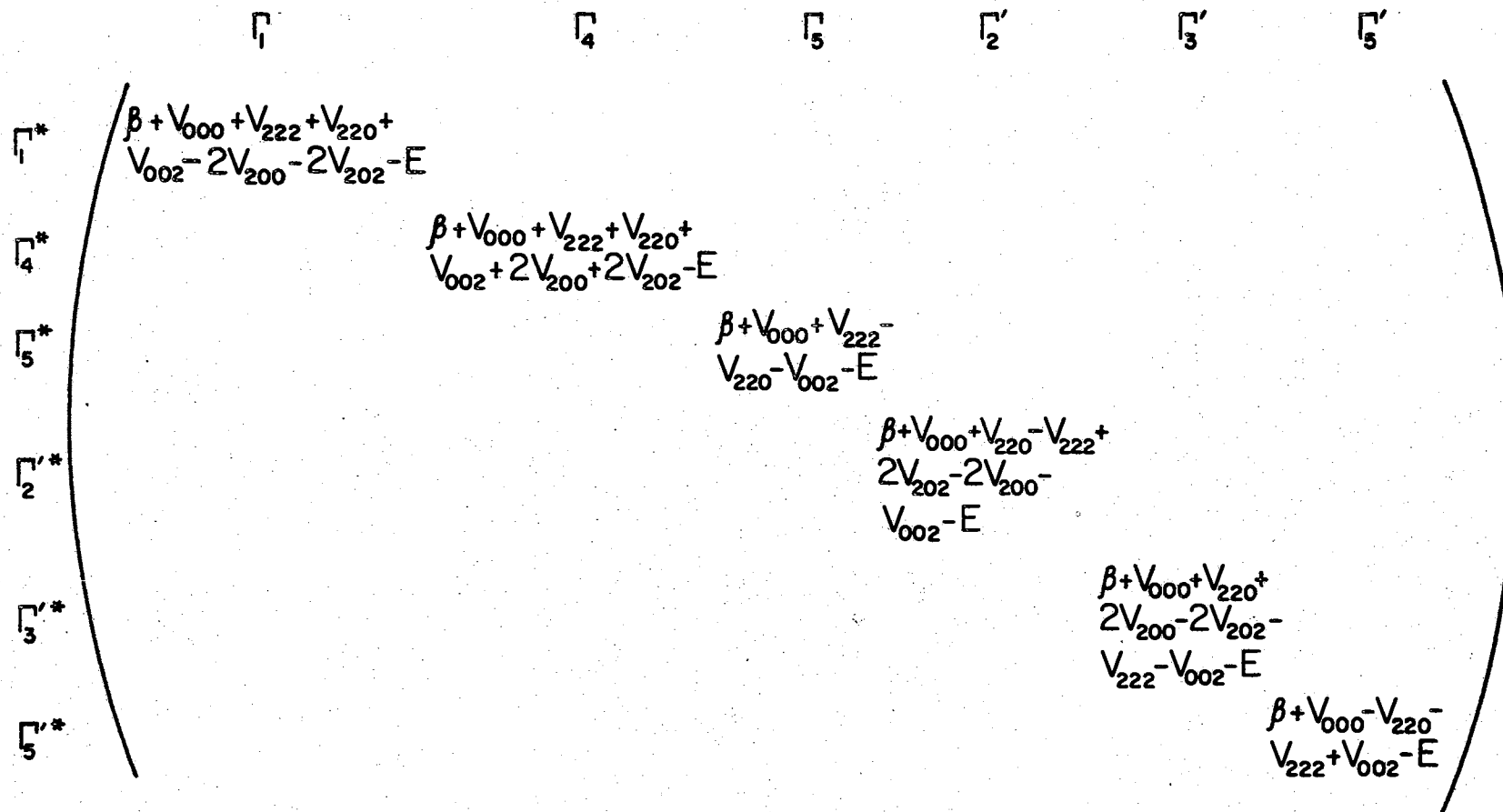
If the set of nineteen plane waves are to be utilized and the secular equation is to be factored, it may be seen that automatically a tremendous simplification occurs due to the orthogonality of the existing irreducible representations. This orthogonality results in the vanishing of all matrix elements between plane waves of unlike symmetry and automatically factors the 19 x 19 secular equation into the form

TABLE V
STANNIC OXIDE WAVEFUNCTIONS

Symmetry	Wavefunction
Γ_1	$1/\sqrt{8} (\langle 111 \rangle + \langle \bar{1}\bar{1}\bar{1} \rangle + \langle \bar{1}\bar{1}1 \rangle + \langle 11\bar{1} \rangle - \langle 1\bar{1}\bar{1} \rangle - \langle \bar{1}11 \rangle - \langle \bar{1}\bar{1}\bar{1} \rangle - \langle 11\bar{1} \rangle)$
Γ_4	$1/\sqrt{8} (\langle 111 \rangle + \langle \bar{1}\bar{1}\bar{1} \rangle + \langle \bar{1}\bar{1}1 \rangle + \langle 11\bar{1} \rangle + \langle 1\bar{1}\bar{1} \rangle + \langle \bar{1}11 \rangle + \langle \bar{1}\bar{1}\bar{1} \rangle + \langle 11\bar{1} \rangle)$
Γ_5	$1/2 \{ (\langle 111 \rangle + \langle \bar{1}\bar{1}\bar{1} \rangle - \langle \bar{1}\bar{1}1 \rangle - \langle 11\bar{1} \rangle); (\langle 1\bar{1}\bar{1} \rangle + \langle \bar{1}\bar{1}\bar{1} \rangle - \langle 1\bar{1}\bar{1} \rangle - \langle \bar{1}\bar{1}\bar{1} \rangle) \}$
$\Gamma_{2'}$	$1/\sqrt{8} (\langle 111 \rangle + \langle \bar{1}\bar{1}\bar{1} \rangle + \langle \bar{1}\bar{1}1 \rangle + \langle 11\bar{1} \rangle - \langle 1\bar{1}\bar{1} \rangle - \langle \bar{1}11 \rangle - \langle 11\bar{1} \rangle - \langle \bar{1}\bar{1}\bar{1} \rangle)$
$\Gamma_{3'}$	$1/\sqrt{8} (\langle 111 \rangle + \langle \bar{1}\bar{1}\bar{1} \rangle + \langle \bar{1}\bar{1}1 \rangle + \langle 11\bar{1} \rangle - \langle 1\bar{1}\bar{1} \rangle - \langle \bar{1}11 \rangle - \langle \bar{1}\bar{1}\bar{1} \rangle - \langle 11\bar{1} \rangle)$
$\Gamma_{5'}$	$1/2 (\langle 111 \rangle - \langle \bar{1}\bar{1}\bar{1} \rangle - \langle \bar{1}\bar{1}1 \rangle + \langle 11\bar{1} \rangle), (\langle 1\bar{1}\bar{1} \rangle - \langle 1\bar{1}\bar{1} \rangle - \langle \bar{1}\bar{1}\bar{1} \rangle + \langle \bar{1}\bar{1}\bar{1} \rangle)$

TABLE VI
DIAMOND WAVEFUNCTIONS

Symmetry	Wavefunction
Γ_1	$1/\sqrt{8} [\langle 111 \rangle - \langle 1\bar{1}\bar{1} \rangle - \langle \bar{1}\bar{1}\bar{1} \rangle - \langle \bar{1}\bar{1}1 \rangle + \langle \bar{1}\bar{1}\bar{1} \rangle - \langle \bar{1}11 \rangle - \langle 1\bar{1}\bar{1} \rangle - \langle 11\bar{1} \rangle]$
$\Gamma_{2'}$	$1/\sqrt{8} [\langle 111 \rangle - \langle 1\bar{1}\bar{1} \rangle - \langle \bar{1}\bar{1}\bar{1} \rangle - \langle \bar{1}\bar{1}1 \rangle - \langle \bar{1}\bar{1}\bar{1} \rangle + \langle \bar{1}11 \rangle + \langle 1\bar{1}\bar{1} \rangle + \langle 11\bar{1} \rangle]$
$\Gamma_{25'}$	$\begin{cases} 1/\sqrt{8} [\langle 111 \rangle + \langle 1\bar{1}\bar{1} \rangle + \langle \bar{1}\bar{1}\bar{1} \rangle - \langle \bar{1}\bar{1}1 \rangle + \langle \bar{1}\bar{1}\bar{1} \rangle + \langle \bar{1}11 \rangle + \langle 1\bar{1}\bar{1} \rangle - \langle 11\bar{1} \rangle] \\ 1/\sqrt{8} [\langle 111 \rangle + \langle 1\bar{1}\bar{1} \rangle + \langle \bar{1}\bar{1}\bar{1} \rangle - \langle \bar{1}\bar{1}1 \rangle + \langle \bar{1}\bar{1}\bar{1} \rangle + \langle \bar{1}11 \rangle + \langle 1\bar{1}\bar{1} \rangle - \langle 11\bar{1} \rangle] \\ 1/\sqrt{8} [\langle 111 \rangle + \langle 1\bar{1}\bar{1} \rangle - \langle \bar{1}\bar{1}\bar{1} \rangle + \langle \bar{1}\bar{1}1 \rangle + \langle \bar{1}\bar{1}\bar{1} \rangle + \langle \bar{1}11 \rangle - \langle 1\bar{1}\bar{1} \rangle + \langle 11\bar{1} \rangle] \end{cases}$
Γ_{15}	$\begin{cases} 1/\sqrt{8} [\langle 111 \rangle + \langle 1\bar{1}\bar{1} \rangle + \langle \bar{1}\bar{1}\bar{1} \rangle - \langle \bar{1}\bar{1}1 \rangle - \langle \bar{1}\bar{1}\bar{1} \rangle - \langle \bar{1}11 \rangle - \langle 1\bar{1}\bar{1} \rangle + \langle 11\bar{1} \rangle] \\ 1/\sqrt{8} [\langle 111 \rangle + \langle 1\bar{1}\bar{1} \rangle - \langle \bar{1}\bar{1}\bar{1} \rangle + \langle \bar{1}\bar{1}1 \rangle - \langle \bar{1}\bar{1}\bar{1} \rangle - \langle \bar{1}11 \rangle + \langle 1\bar{1}\bar{1} \rangle - \langle 11\bar{1} \rangle] \\ 1/\sqrt{8} [\langle 111 \rangle - \langle 1\bar{1}\bar{1} \rangle + \langle \bar{1}\bar{1}\bar{1} \rangle + \langle \bar{1}\bar{1}1 \rangle - \langle \bar{1}\bar{1}\bar{1} \rangle + \langle \bar{1}11 \rangle - \langle 1\bar{1}\bar{1} \rangle - \langle 11\bar{1} \rangle] \end{cases}$



$$\beta = 4.23 = l_1^2 + l_2^2 + l_3^2 (a/c)^2$$

Figure 12. Factored (111) Secular Equation for the Stannic Oxide Structure

$$\begin{array}{cccc}
 & \Gamma_1 & \Gamma_2' & \Gamma_{25}' & \Gamma_{15} \\
 \Gamma_1^* & \left(\begin{array}{c} \beta + V_{000} + V_{222} + \\ 3V_{220} - E \end{array} \right. & & & \\
 \Gamma_2'^* & & \left(\begin{array}{c} \beta + V_{000} + 3V_{220} \\ -V_{222} - E \end{array} \right. & & \\
 \Gamma_{25}'^* & & & \left(\begin{array}{c} \beta + V_{000} - V_{220} \\ +V_{222} - E \end{array} \right. & \\
 \Gamma_{15}^* & & & & \left. \begin{array}{c} \beta + V_{000} - V_{220} \\ -V_{222} \end{array} \right)
 \end{array}$$

$$\beta = 3.0 = l_1^2 + l_2^2 + l_3^2$$

Figure 13. Factored (111) Secular Equation for the Diamond Structure.

TABLE VII
FREE ELECTRON ENERGY EIGENVALUES AND THEIR CORRESPONDING
SYMMETRIZED COMBINATIONS OF PLANE WAVES

Plane Wave Group	Free Electron Energy	Symmetrized Combination of Plane Waves (SCPW)
$\langle 000 \rangle$	0	$\Gamma_1 = \langle 000 \rangle$
$(100)(010)(100)(010)$	1.0 (Rydbergs)	$\Gamma_2 \rightarrow \frac{1}{2} (100 + \bar{1}00 - 0\bar{1}0 - 010)$ $\Gamma_4 \rightarrow \frac{1}{2} (100 + \bar{1}00 + 0\bar{1}0 + 010)$ $\Gamma_5 \rightarrow 1/\sqrt{2} (100 - \bar{1}00, 010 - 0\bar{1}0)$
$(110), (110), (110), (110)$	2.0 Rydbergs	$\Gamma_1 \rightarrow \frac{1}{2} (110 + \bar{1}\bar{1}0 + \bar{1}10 + \bar{1}\bar{1}0)$ $\Gamma_4 \rightarrow \frac{1}{2} (110 + \bar{1}\bar{1}0 - \bar{1}10 - 1\bar{1}0)$ $\Gamma_5 \rightarrow 1/\sqrt{2} [(110 - \bar{1}\bar{1}0), (1\bar{1}0 - \bar{1}10)]$
$(001), (001)$	$(a/c)^2 = 2.23$ Rydbergs	$\Gamma_4 \rightarrow 1/\sqrt{2} [(001) + (00\bar{1})]$ $\Gamma_3' \rightarrow 1/\sqrt{2} [(001) - (00\bar{1})]$
$(011)(101)(011)(011)$ $(101)(101)(011)(101)$	3.23 Rydbergs	$\Gamma_1 \rightarrow 1/\sqrt{8} [011 + 101 + 0\bar{1}1 + 01\bar{1} + \bar{1}01 + 10\bar{1} + 0\bar{1}\bar{1} + \bar{1}0\bar{1}]$ $\Gamma_3 \rightarrow 1/\sqrt{8} [011 + 0\bar{1}1 - \bar{1}01 - 101 + 01\bar{1} + 0\bar{1}\bar{1} - \bar{1}0\bar{1} - 10\bar{1}]$ $\Gamma_5 \rightarrow \left(\frac{011 - 0\bar{1}1 + 0\bar{1}\bar{1} - 01\bar{1}}{2}, \frac{101 - \bar{1}01 + \bar{1}0\bar{1} - 10\bar{1}}{2} \right)$ $\Gamma_2' \rightarrow 1/\sqrt{8} [011 + 0\bar{1}1 + 101 + \bar{1}01 - 01\bar{1} - 0\bar{1}\bar{1} - \bar{1}0\bar{1} - 10\bar{1}]$ $\Gamma_4' \rightarrow 1/\sqrt{8} [011 + 0\bar{1}1 - 101 - \bar{1}01 - 01\bar{1} - 0\bar{1}\bar{1} + \bar{1}0\bar{1} + 10\bar{1}]$ $\Gamma_5' \rightarrow \left(\frac{011 - 0\bar{1}1 - 0\bar{1}\bar{1} + 01\bar{1}}{2}, \frac{101 - \bar{1}0\bar{1} - \bar{1}01 + 10\bar{1}}{2} \right)$

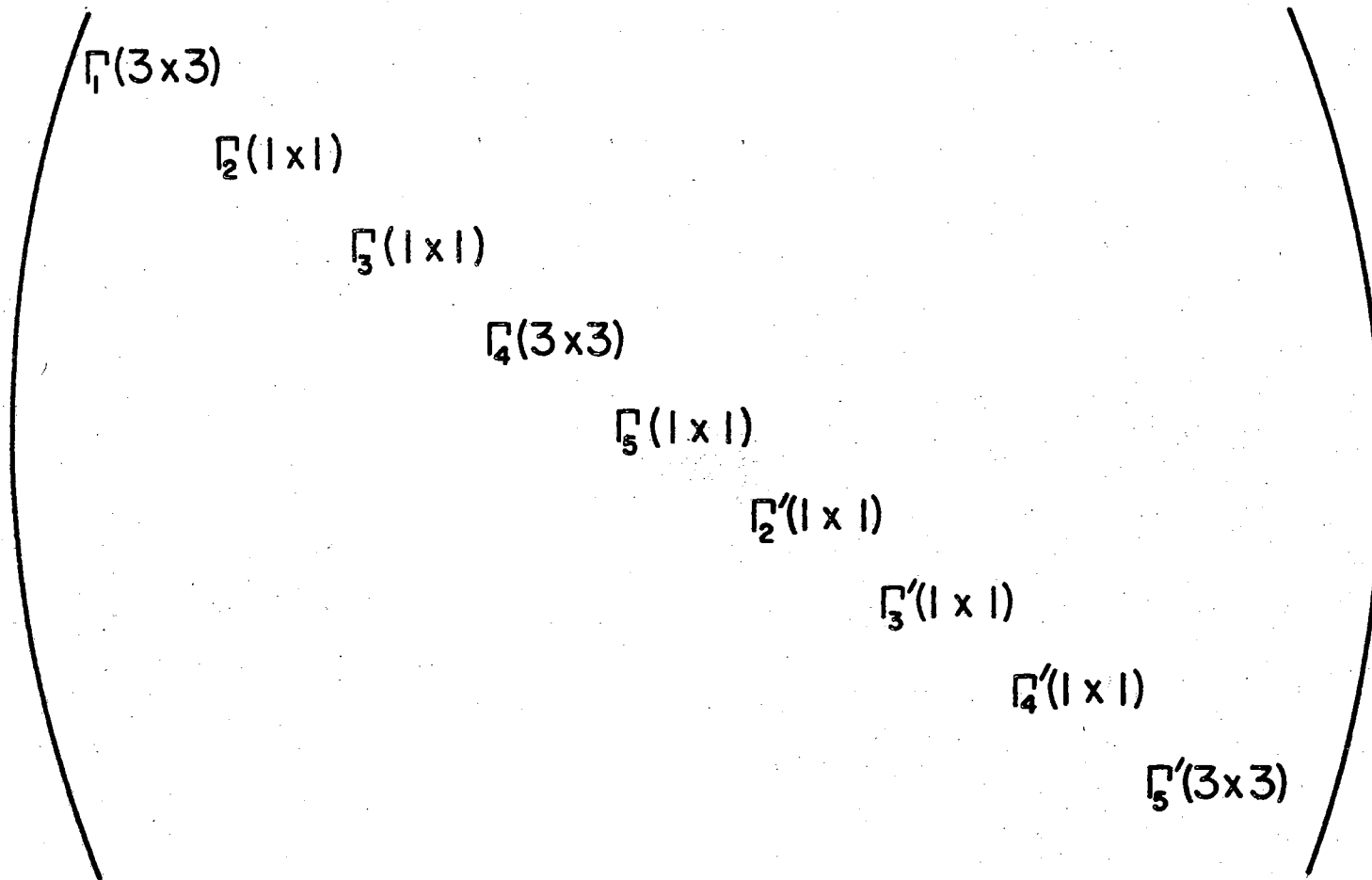


Figure 14. Schematic Representation of the Factored Secular Equation Applicable to the Stannic Oxide Structure Using Nineteen Plane Waves

$$\begin{pmatrix}
 \beta_{000} + V_{000} - E & 2V_{110} & 2\sqrt{2}V_{101} \\
 2V_{110} & \beta_{110} + V_{000} + 2V_{200} + V_{220} - E & (V_{121} + V_{101})2\sqrt{2} \\
 2\sqrt{2}V_{101} & 2\sqrt{2}(V_{101} + V_{121}) & \beta_{011} + V_{000} + 2V_{110} - V_{120} + 2V_{112} + V_{002} + V_{202} - E
 \end{pmatrix} \square_1$$

$$\begin{pmatrix}
 \beta_{100} + V_{000} + V_{200} - 2V_{110} - E \\
 \beta_{011} - E + V_{000} + V_{200} - 2V_{112} \\
 -2V_{110} + V_{002} + V_{202}
 \end{pmatrix} \begin{matrix} \square_2 \\ \square_3 \end{matrix}$$

$$\begin{pmatrix}
 \beta_{100} - E + V_{000} + V_{200} + 2V_{110} & \sqrt{2}V_{120} & 2\sqrt{2}V_{101} \\
 \sqrt{2}V_{120} & \beta_{110} - E + V_{000} + V_{220} - 2V_{200} & 2\sqrt{2}V_{111} \\
 2\sqrt{2}V_{101} & 2\sqrt{2}V_{111} & \beta_{001} + V_{000} + V_{002}
 \end{pmatrix} \square_4$$

$$\begin{pmatrix}
 \beta_{011} - E + V_{000} - V_{200} + V_{202} - V_{002} \\
 \beta_{011} - E + V_{000} + V_{200} + 2V_{110} \\
 -V_{002} - V_{202} - 2V_{112} \\
 \beta_{001} - E + V_{000} - V_{002}
 \end{pmatrix} \begin{matrix} \square_5 \\ \square_2' \\ \square_3' \end{matrix}$$

$$\begin{pmatrix}
 \beta_{100} + V_{000} - V_{200} - E & -\sqrt{2}V_{120} & -2\sqrt{2}V_{111} \\
 -\sqrt{2}V_{120} & \beta_{110} - E + V_{000} - V_{220} & \sqrt{2}(V_{101} - V_{121}) \\
 -2\sqrt{2}V_{111} & \sqrt{2}(V_{101} - V_{121}) & \beta_{011} - E + V_{000} - V_{200} - V_{202} + V_{002}
 \end{pmatrix} \square_5'$$

$$\begin{pmatrix}
 \beta_{011} + V_{000} + V_{200} - 2V_{110} - V_{002} \\
 -V_{202} + 2V_{112} - E
 \end{pmatrix} \square_4'$$

$$\beta_{1,1,2,3} = l_1^2 + l_2^2 + l_3^2 (a/c)^2$$

Figure 15. Components of the Secular Equation Illustrated in Figure 14

shown in Figure 14. Extension to the 55 x 55 secular equation follows the same procedure but includes all plane waves up through a free electron energy of 7.23 Rydbergs.

Leaving the center of the zone and considering an axial wave vector group, it is necessary to follow the same procedures. However, due to the reduced symmetry of these groups, the block diagonal matrices are of a relatively large order when compared with those at the center of the zone.

Considering the matrices for the center of the zone and for any axial wavevector group which has states compatible with center-zone states, it is evident that if the concept of continuity is to be maintained, the energies calculated for the compatible electronic states at the center of the zone must be the same. Unfortunately, due to the lack of an infinite number of plane waves in the calculation, this is seldom the case. As a result, the number of plane waves is fixed, the energies are calculated for compatible states and compared. If agreement is not evident to within a few electron volts, the oxygen form factor must be changed. Thus, using the criterion of compatibility, the location of the oxygen form factor may be ascertained to a first approximation.

At first glance, the means of reading some physical significance into the resultant situation would involve finding the inverse Fourier transform of the resultant form factors. This Fourier transform should have some meaning if a one-electron potential is to be calculated. However, such action should be taken with a great deal of caution because the resultant configuration of form factors has meaning only in that it is this set that allows the calculation to proceed on the basis

of matching the energies of compatible electron states. As a result, this set of form factors implicitly rather than explicitly contains such things as electron-electron interactions, exchange, electron-nuclear interactions, and many other effects often brought into a "first principles" calculation. The difficulty herein is that the relative strength of each of these effects remains unknown.

CHAPTER VI

DISCUSSION OF RESULTS

In this first effort at making an energy band calculation for stannic oxide, primary emphasis has been placed upon developing the theory in terms of a local pseudopotential formalism. This has been done to test the practical utility and consequent desirability for application of this type of treatment to the crystal system at hand. For example, it was considered important to get an estimate for a lower limit to the size of the plane-wave approximation necessary to obtain consistent results. Another area of interest involved setting forth suitable criteria for examining the validity of the local approximation and for determining the best locations of the tin and oxygen form factors based on continuity of the wavefunctions and matching of compatible electronic state energies at both the zone center and zone boundary. As will be seen below, the calculation as performed has made emphatic the limitations of the method and of the approximations used. It has, however, also made it possible to identify the logical next steps which should be taken in future calculations designed to refine the rudimentary band structure as obtained so that it can be subjected to realistic comparison with experimental data.

The calculation attempted had its basis in a self-consistent, yet empirical, technique. The method used is self-consistent since the location of the oxygen form factor was determined by adjusting its posi-

tion until compatible electronic states at $\underline{k} = 0$ had the same energy. However, the method is empirical because no attempt was made to consider the effect of the existence of the oxygen valence electrons and their contribution to the pseudopotential.

The general procedures outlined during the earlier chapters of this report are valid regardless of the crystal space group and ion species within the crystal. However, the fact must be accepted that there are stringent limitations to the range of validity of results acquired using a local approximation. In particular, the mixing of electronic states for $\underline{k} \neq 0$ is of major concern. For a treatment of this topic, the reader is referred to Kleinman and Phillips (55). Unless appropriate mixing is taken into account, severe discrepancies between theory and experiment are to be expected. This mixing of states may best be considered within the framework of 2nd order perturbation theory. Unless such precautions are taken, incorrect symmetry classification of allowed electron states. Due to the lack of the inclusion of the mixing leads to what is actually an incorrect potential for any point other than that at the center of the zone. Therefore, the resultant bands can be correctly classified within the framework of the theory being used yet incorrectly classified when compared to similar bands acquired after a "better" calculation is made. However, for this first calculation, it was decided that the utilization of 2nd order effects was premature.

Another important consideration is the fixing of a lower limit to the size of the plane-wave approximation. A usual procedure is to plot electronic state energies obtained at each symmetry point as a function of the number of plane-waves used in the calculation. When this curve levels for the least symmetric state it has in general already leveled

for states of a higher symmetry. Prior calculations utilizing such a criterion (64) have been carried out for cubic systems. The results presented here coupled with those of Staflen, et.al. (75) now suggest that it may be necessary to consider as many as two-hundred plane-waves to obtain the desired consistency for stannic oxide.

With such a procedure it has been noted that in general, the more symmetric states, i.e. those obtained using the wavevector groups of highest order, converge to a final energy more quickly than do other states. Consequently, the calculation as performed should have a somewhat greater degree of validity at the center of the zone than elsewhere. For this reason the agreement between compatible electronic states energies at this point appears to be a good criterion for determining the validity of such local approximation. At the center of the zone, the largest observed discrepancy between compatible electronic state energies was less than three electron volts. However, discrepancies as large as six and one-half electron volts occurred at the zone edge. This added amount of error has two different sources. The lack of a consideration a 2nd order effects is made evident by the nonvanishing overlaps of plane-waves of different symmetry classifications.

Thus, the bands which result must be scrutinized very closely along a symmetry axis to see if they have the proper definition. In addition, the mixing of atomic-like states has been ignored as mentioned above and this can also contribute to the increased error as the zone edge is approached. Despite the problems encountered, the calculation done appears to have some merit in a qualitative sense, since it illustrates the existence of some definite energy bands and predicts the presence of at least one large forbidden energy gap. As has been re-

peatedly emphasized, however, neither band shapes nor energy separations should be interpreted quantitatively at this time. The bands obtained are illustrated in Figure 16 and were acquired by considering the nearly-free electron energies at the surface of the zone (X point), symmetry classifying the resultant eigenvectors, and matching states of the same symmetry by taking a simple average of the two energies which arose. The same procedure was followed with regard to compatible states at the center of the zone, although averaging was less important because the basic agreement was better. However, due to the mixing of atomic states, the size of the approximation being used, and the uncertainty in the relative location of the two resultant form factor curves, the axial calculations were of little use other than to indicate a lack of structure between Γ and X. Any structure shown was introduced to insure that at the center of the zone and at the zone edge, the bands should have zero slope and thus be essentially parallel. Since the bands in Figure 15 were drawn using only the energies at these two points and symmetry classified through a knowledge of the compatibility relations between electronic states the reader should realize that they must be accepted only as a point of departure for improved calculations. There are two obvious indications that the bands as shown are not representative of the true physical situation: First, they have a center-zone forbidden gap separation which does not agree with experimentally observed band gaps or reflectance data. Secondly, they do not fulfill the usual condition that the uppermost valence band and lowest conduction band states have the highest degree of degeneracy possible within the space group.

At this stage it would seem appropriate to outline a method by

which the results of a calculation similar to that already discussed may be improved and brought into ultimate agreement with experimental observations:

- 1) Calculate the energies of compatible states at the center of the zone using only 55 plane-waves while taking into consideration 2nd order perturbation theory. Do this so the difference in energy between them is less than one electron volt for every energy of interest.
- 2) Check this calculation by considering the axial bands which arise and the agreement between compatible electronic states occurring at the zone edge. If there is good agreement between these energies it may be assumed that the axial calculation has some degree of validity.
- 3) Assuming that these criteria have been met, the next step is to consider the separation in energy between valence and conduction bands and attempt to correlate this result with experiment.
- 4) If correlation between theory and experiment is poor, (i.e., if the difference between allowed electron energies at the center of the zone does not agree with that observed optically) the next step is to change the position of the tin form factor. As an illustrative example, suppose this is indeed the case. The tin form factor would then be moved to the left by one unit and the calculation repeated for a range of oxygen form factor positions. When the resultant new set of bands is acquired it should also be compared with the experimental criterion mentioned. If the amount of disagreement is lessened, the pro-

cedure is evident. Simply move the tin form factor even further in the same direction. However, if the disagreement is increased, move the tin form factor in the opposite direction and reconsider the calculation.

- 5) If it becomes impossible to match energies of compatible states at either zone center or zone boundary, or if a good match is achieved but the bandgap is of an obviously incorrect magnitude, increase the size of the plane-wave approximation and again follow the procedure outlined above.

Once this total procedure has been followed, and a set of bands has been acquired having proper separation in energy, the pseudopotential coefficients used to obtain these bands should be further utilized to make corresponding calculations along the other symmetry axes. These should provide better insight from a purely theoretical point of view as to the energetically possible direct and indirect transitions which can arise in the crystal. Of course, it is to be expected that the resultant calculation along all possible symmetry axes will lead to a complete definition of the existing reflectance spectrum. This calculation should also indicate that there are some other possible transitions which are of importance but are of an energy beyond the present experimentally investigated region of the reflectance spectrum.

The validity of these bands may also be checked in another unique way. This method has been utilized by others (67, 71) and consists of calculating the imaginary part of the complex dielectric constant via a Kramers-Kronig type analysis which utilized energies that are acquired directly from the calculated bands. If the obtained curve of ϵ_2 vs energy compares with the reflectance spectrum acquired experimen-

tally, there must be little doubt that the bands are essentially correct.

One of the goals of this work was to correlate the experimental reflectance data given in Figures 7 and 8 with the band structure calculation. It is evident from the previous discussion that such a correlation based on Figure 16 would have no intrinsic value. In anticipation of improved bands based on future calculation refinements, however, selection rules for polarization-dependent and polarization-independent direct optical transitions at important symmetry points have been derived and are tabulated in Appendix III.

In perspective it must be realized that a complete and satisfying band structure calculation for stannic oxide still lies some distance in the future. It now seems clear, however, that fruitful results can be obtained by following the pseudopotential approach, improving the approximations, including 2nd order perturbation theory, and increasing the number of plane-waves considered.

CHAPTER VII

SUGGESTIONS FOR FURTHER STUDY

There are many different areas in which further study would be beneficial. Phillips (10) mentions some new and more fruitful means for experimentally studying solids and their reflectance spectra. Since the entire body of knowledge in this area has been mainly applied to cubic systems and the study of such effects for systems of a reduced symmetry has not been thoroughly exploited, many questions pertaining to the interpretation of experimental effects require additional investigation.

There is a definite need to extend the specific experimental investigation described in this paper. In particular, the monochromator as built has in it an inherent flexibility which allows for further work on the optical properties of materials. Future measurements should seek reflectance data at reduced temperatures, increased photon energies, and higher levels of light intensity. In each instance the reflectance spectra should be subjected to a complete Kramers-Kronig analysis in order to gain increased insight regarding the energies of electron transitions.

Regarding the band structure calculation, it is quite evident that further work in this area is a must if any consistent means of symmetry classifying electron transitions is to be attempted. In addition, to immediate refinements which were outlined in detail in the last chapter,

a band structure should also be acquired using an OPW or APW calculation so the similarities and differences between this type of approach and an empirical pseudopotential treatment can be ascertained. In either case, there is now strong evidence that the c-axis tin-tin interaction is of a sufficient order of magnitude to warrant study of the bands in terms of an approach which utilizes a Hamiltonian containing this interaction. In this respect, the work of Weisz (70) could prove quite helpful.

BIBLIOGRAPHY

1. E. E. Kohnke, J. Phys. Chem. Solids 23, 1557 (1962).
2. S. F. Reddaway & D. A. Wright, Brit. J. Appl. Phys. 16, 195 (1965).
3. H. Kunkle and E. E. Kohnke, J. Appl. Phys. 36 #4, 1489 (1965).
4. K. Ishiguro, T. Sasaki, T. Arai, and I. Imai, Journal of the Physical Society of Japan 13 #3, 296 (1958).
5. S. F. Reddaway, Brit. J. Appl. Phys. 17, 697 (1966).
6. J. A. Marley and R. C. Dockerty, Phys. Rev. 140, A304 (1965).
7. L. Van Hove, Phys. Rev. 89, 1189 (1953).
8. J. C. Phillips, J. Phys. Chem. Solids 8, 369 (1959).
9. D. Brust, Phys. Rev. 139 #2, A489 (1965).
10. J. C. Phillips, "The Fundamental Optical Spectra of Solids", Solid State Physics 18, 56 (1966).
11. F. Abeles, Optical Properties and Electronic Structure of Metals and Alloys, Proceedings of the International Colloquium held at Paris 13-16 September 1965, John Wiley & Sons, Inc., New York (1966).
12. T. S. Moss, Optical Properties of Semiconductors, Academic Press Inc., New York (1959).
13. M. Sachs, Solid State Theory, McGraw-Hill Book Co. Inc., New York, (1963).
14. C. Kittel, Introduction to Solid State Physics, John Wiley & Sons Inc., (1956).
15. R. A. Houston, Treatise on Light, Longmans Inc., London (1938).
16. R. H. Bube, Photoconductivity of Solids, John Wiley & Sons, Inc., New York (1960).
17. F. Seltz, The Modern Theory of Solids, McGraw-Hill Inc., New York, (1940).

18. J. A. Stratton, Electromagnetic Theory, McGraw-Hill Inc., New York, (1941).
19. Stern, Phys. Rev. 133 #6, A1653 (1964).
20. M. Cardona, Phys. Rev. 129 #1, 69 (1963).
21. M. Cardona and D. L. Greenway, Phys. Rev. 133 #6, A1685 (1964).
22. H. R. Philipp and H. Ehrenreich, Phys. Rev. 129 #4, 1550 (1963).
23. H. R. Philipp and H. Ehrenreich, Phys. Rev. 137 #5, 2016 (1963).
24. P. M. Lee, Phys. Rev. 135 #4, A1110 (1964).
25. H. R. Philipp and E. H. Taft, Phys. Rev. 113, 1002 (1959).
26. J. C. Phillips, Phys. Rev. 104, 1263 (1956).
27. Walker and J. F. Osantowski, Phys. Rev. 134 #1, A153 (1964).
28. H. R. Philipp and E. H. Taft, Phys. Rev. 113 #4, 1002 (1959).
29. H. R. Philipp and E. H. Taft, Phys. Rev. 120 #1, 37 (1960).
30. H. R. Philipp and E. H. Taft, Phys. Rev. 127 #1, 159 (1962).
31. B. Lax, Rev. Mod. Physics 30 #1, 122 (1958).
32. J. C. Phillips, H. R. Philipp, and H. Ehrenreich, Phys. Rev. Letters 8 #2, 59 (1962).
33. J. C. Phillips, Phys. Rev. 133 #2, A452 (1964).
34. L. F. Mattheiss, Phys. Rev. 134 #4, A970 (1964).
35. M. L. Cohen, and T. K. Bergstresser, Phys. Rev. 141 #2, 789 (1966).
36. M. Cardona and G. Harbeke, Phys. Rev. 137 #5, A1467 (1965).
37. P. D. Johnson, J. Opt. Soc. 42, 278 (1952).
38. W. W. Parkinson, Jr., and F. E. Williams, J. Opt. Soc. 89, 705 (1949).
39. P. D. Johnson, Rev. Sci. Instrument 28 #10, 833 (1957).
40. R. Allison, J. Burns, and A. J. Tuzzolino, J. Opt. Soc. 54, 1381 (1964).
41. R. Allison, J. Burns, and A. J. Tuzzolino, J. Opt. Soc. 54, 747 (1964).

42. H. R. Philipp and H. Ehrenreich, Phys. Rev. 129 #4, 1550 (1963).
43. S. Huang, "Refractive Indices of Cassiterite", M.S. Thesis, Oklahoma State University, Stillwater, Oklahoma, May (1963).
44. H. Kunkle and E. E. Kohnke, J. Appl. Phys. 36, 1489 (1965).
45. M. Cardona and D. L. Greenway, Phys. Rev. 131, 98 (1963).
46. H. Kunkle, "High Temperature Conductivity of Grown Stannic Oxide Single Crystals", Ph.D. Dissertation, Oklahoma State University, Stillwater, Oklahoma, May (1966).
47. L. Pincherle, "Band Structure Calculations in Solids", Reports on Progress in Physics.
48. J. Callaway, Energy Band Theory, Academic Press, New York, (1964).
49. W. Harrison, Pseudopotentials in the Theory of Metals, W. A. Benjamin Inc., New York (1966).
50. E. I. Blount, Solid State Physics 13, Academic Press, New York (1962).
51. H. Jones, The Theory of Brillouin Zones and Electronic States in Crystals, North Holland Publishing Co., Amsterdam (1962).
52. F. Herman, Rev. Mod. Phys. 30, 102 (1958).
53. A. Nussbaum, Solid State Physics Vol. 18, Academic Press, New York (1966).
54. J. C. Phillips, J. Phys. Chem. Solids 8, 369 (1959).
55. J. C. Phillips and L. Kleinman, Phys. Rev. 116 #2, 287 (1959).
56. F. Bassani and V. Celli, J. Phys. Chem. Solids 20, 64 (1961).
57. W. A. Harrison, Phys. Rev. 126 #2, 497 (1962).
58. R. S. Knox and F. Bassani, Phys. Rev. 124 #3, 652 (1961).
59. B. J. Austin, V. Heine, and L. J. Sham, Phys. Rev. 127 #1, 276 (1962).
60. A. J. Hughes and J. Callaway, Phys. Rev. 136 #5, A1390 (1964).
61. L. M. Falicov and P. J. Lin, Phys. Rev. 141 #2, 562 (1966).
62. P. J. Lin and L. M. Falicov, Phys. Rev. 142 #2, 441 (1966).
63. P. J. Lin and L. Kleinman, Phys. Rev. 142 #2, 478 (1966).
64. M. L. Cohen and T. K. Bergstresser, Phys. Rev. 141 #2, 789 (1966).

65. L. Kleinman and J. C. Phillips, Phys. Rev. 118 #5, 1153 (1960).
66. F. Bassani and D. Brust, Phys. Rev. 131 #4, 1524 (1963).
67. D. Brust, Phys. Rev. 134 #5, A1337 (1964).
68. W. A. Harrison, Phys. Rev. 118, #5, 1182 (1960).
69. J. R. Anderson and A. V. Gold, Phys. Rev. 139 #5, A1459 (1965).
70. G. Weisz, Phys. Rev. 149 #2, 504 (1966).
71. M. L. Cohen and P. J. Lin, Phys. Rev. 155, #3, 992 (1967).
72. F. Herman and S. Skillman, Atomic Structure Calculations, Prentice-Hall, Inc., Englewood Cliffs, New Jersey (1963).
73. F. Herman, Dissertation (Unpublished), Columbia University, January 1953.
74. R. G. W. Wyckoff, Crystal Structures, Interscience, New York (1951).
75. M. D. Stafleu, Phys. Status Solidi 23 #2, 67 (1967).
76. J. C. Slater, Quarterly Progress Report Number 48, April 15, 1963, Solid State and Molecular Theory Group, Massachusetts Institute of Technology, Cambridge, Massachusetts.
77. K. Olbrychski, Phys. Status Solidi 3, 2155 (1963).
78. B. P. Clark, "Application of the Free Electron Approximation to the Structural Space Group D_{4h}^{14} ", Master's Thesis, Oklahoma State University, Stillwater, Oklahoma (1964).
79. H. A. Bethe, Ann. Physik 3, 133 (1929).
80. W. Opechowski, Physica 7, 552 (1940).
81. R. J. Elliott, Phys. Rev. 96, 280 (1954).
82. E. Wigner, Göttingen Nachr. 546 (1932).
83. C. Herring, Phys. Rev. 52, 361 (1937).
84. M. Lax and J. J. Hopfield, Phys. Rev. 124, 115 (1961).

APPENDIX A

SINGLE GROUP ANALYSIS

Character systems for the D_{4h}^{14} space group given by Slater (76) and derivable from generators published by Olbryskii (77) show some disagreement at a few points in the first Brillouin zone. A prior report (78) on this project mentioned that the characters of the various wavevector groups could be extracted rather quickly and gave a tabulation which has now been discovered to contain errors at three symmetry points. To remove confusion, a complete and corrected set of characters for this system is given below. It should be emphasized that this set is in agreement with the work of Olbryskii.

The first table indicates (using the notation of the first report (78)), the wavevector group associated with each symmetry point, the set of elements in each group, and the table which contains the characters appropriate to this particular wavevector group. The following ten tables contain the character systems and Table XII contains the compatibility relations which may be extracted simply by matching characters of compatible electronic states. For more detail as to the reason for, and means of, extracting the compatibility relations, the reader is referred to Jones (51).

TABLE VIII

CLASSES AND WAVE VECTOR GROUP ELEMENTS AT Γ , A, M, Z, X, R, \mathcal{L} , U, W, S, \mathcal{L} , Δ , V, Y, T

Symmetry Point	Classes	Table
Γ	$C_1 = E, C_2 = C_2, C_3 = T_{mm_1} + T_{mm_2}, C_4 = T_{mJ} + T_{mm_3}, C_5 = R_1 + R_2, C_6 = J, C_7 = m_3, C_8 = T_{mR_1} + T_{mR_2},$ $C_9 = T_m + T_m C_2, C_{10} = m_1 + m_2$	IX
A	$C_1 = E, C_2 = T_{mm_3} + Q T_{mm_3} + T_{mJ} + Q T_{mJ}, C_3 = C_2, C_4 = Q R_1 + R_2, C_5 = T_{mm_1} + Q T_{mm_1} + T_{mm_2} + Q T_{mm_2},$ $C_6 = m_3 + Q m_3, C_7 = T_m + Q T_m + T_m C_2 + Q T_m C_2, C_8 = J + Q J, C_9 = m_1 + m_2, C_{10} = T_{mR_1} + T_{mR_2} + Q T_{mR_1} + Q T_{mR_2},$ $C_{11} = Q m_1 + Q m_2, C_{12} = R_1 + Q R_2, C_{13} = Q C_2, C_{14} = Q$	X
M	$C_1 = E, C_2 = C_2, C_3 = T_{mm_3} + T_{mJ}, C_4 = T_{mm_2} + T_{mm_1}, C_5 = R_1 + R_2, C_6 = Q, C_7 = Q C_2, C_8 = Q T_{mm_3} + Q T_{mJ},$ $C_9 = Q T_{mm_2} + Q T_{mm_1}, C_{10} = Q R_1 + Q R_2, C_{11} = J, C_{12} = m_3, C_{13} = T_m + T_m C_2, C_{14} = T_{mR_1} + T_{mR_2}, C_{15} = m_1 + m_2,$ $C_{16} = Q J, C_{17} = Q m_3, C_{18} = Q T_m + Q T_m C_2, C_{19} = Q T_{mR_1} + Q T_{mR_2}, C_{20} = Q m_1 + Q m_2$	XI
Z	Same as A	X
X	$C_1 = E, C_2 = Q, C_3 = T_m + Q T_m, C_4 = J + Q J, C_5 = T_{mJ} + Q R_{mJ}, C_6 = m_3, C_7 = Q m_3, C_8 = T_{mm_3} + Q T_{mm_3},$ $C_9 = C_2 + Q C_2, C_{10} = T_m C_2 + Q T_m C_2$	XII
R	$C_1 = E, C_2 = Q, C_3 = T_m + Q T_m, C_4 = m_3 + Q m_3, C_5 = T_{mm_3} + Q T_{mm_3}, C_6 = J, C_7 = Q J, C_8 = T_{mJ} + Q T_{mJ},$ $C_9 = C_2 + Q C_2, C_{10} = T_m C_2 + Q T_m C_2$	XII

TABLE VIII (CONT'D)

Symmetry point	Classes	Table
Λ	$\underline{C}_1 = E, \underline{C}_2 = C_2, \underline{C}_3 = m_1 + m_2, \underline{C}_4 = Tmm_1 + Tmm_2, \underline{C}_5 = Tm + TmC_2$	VIII
U	$\underline{C}_1 = E, \underline{C}_2 = Q, \underline{C}_3 = m_3 + Qm_3, \underline{C}_4 = TmC_2 + QTmC_2, \underline{C}_5 = Tmm_3 + TmJ$	IX
W	$\underline{C}_1 = E, \underline{C}_2 = Q, \underline{C}_3 = C_2 + QC_2, \underline{C}_4 = Tm + QTm, \underline{C}_5 = TmC_2 + QTmC_2$	IX
S, Σ	$\underline{C}_1 = E, \underline{C}_2 = m_2, \underline{C}_3 = R_2, \underline{C}_4 = m_3$	X
Δ	$\underline{C}_1 = E, \underline{C}_2 = m_3, \underline{C}_3 = TmJ, \underline{C}_4 = TmC_2$	X
V	$\underline{C}_1 = E, \underline{C}_2 = C_2, \underline{C}_3 = Tm + TmC_2, \underline{C}_4 = Tmm_1 + Tmm_2, \underline{C}_5 = m_1 + m_2, \underline{C}_6 = Q, \underline{C}_5 + j = QC_5$	XI
Y	$\underline{C}_1 = E, \underline{C}_2 = m_3, \underline{C}_3 = Tm, \underline{C}_4 = Tmm_3$	X
T	$\underline{C}_1 = E, \underline{C}_2 = Q, \underline{C}_3 = m_3 + Qm_3, \underline{C}_4 = Tm + QTm, \underline{C}_5 = Tmm_3 + QTmm_3$	IX

TABLE IX
CHARACTERS AT Γ

	\underline{C}_1	\underline{C}_2	\underline{C}_3	\underline{C}_4	\underline{C}_5	\underline{C}_6	\underline{C}_7	\underline{C}_8	\underline{C}_9	\underline{C}_{10}	Point Symmetry Type
Γ_1	1	1	1	1	1	1	1	1	1	1	$1 + \frac{1}{2}(x^2 + y^2) - z^2$
Γ_2	1	1	1	-1	-1	1	1	1	-1	-1	$xy (x^2 - y^2)$
Γ_3	1	1	-1	1	-1	1	1	-1	1	-1	$x^2 - y^2$
Γ_4	1	1	-1	-1	1	1	1	-1	-1	1	xy
Γ_5	2	-2	0	0	0	2	-2	0	0	0	(yz, xz)
Γ_1'	1	1	1	1	1	-1	-1	-1	-1	-1	$xyz (x^2 - y^2)$
Γ_2'	1	1	1	-1	-1	-1	-1	-1	1	1	z
Γ_3'	1	1	-1	1	-1	-1	-1	1	-1	1	xyz
Γ_4'	1	1	-1	-1	1	-1	-1	1	1	-1	$z (x^2 - y^2)$
Γ_5'	2	-2	0	0	0	-2	2	0	0	0	(x, y)

TABLE X
CHARACTERS AT A

	<u>C</u> ₁	<u>C</u> ₂	<u>C</u> ₃	<u>C</u> ₄	<u>C</u> ₅	<u>C</u> ₆	<u>C</u> ₇	<u>C</u> ₈	<u>C</u> ₉	<u>C</u> ₁₀	<u>C</u> ₁₁	<u>C</u> ₁₂	<u>C</u> ₁₃	<u>C</u> ₁₄
	1	1	1	1	1	1	1	1	1	1	1	1	1	1
	1	1	1	-1	-1	1	1	1	-1	-1	-1	-1	1	1
	1	-1	1	-1	1	1	-1	1	-1	1	-1	-1	1	1
	1	-1	1	1	-1	1	-1	1	1	-1	1	1	1	1
	2	0	-2	0	0	2	0	-2	0	0	0	0	-2	2
	1	1	1	1	1	-1	-1	-1	-1	-1	-1	1	1	1
	1	1	1	-1	-1	-1	-1	-1	1	1	1	-1	1	1
	1	-1	1	-1	1	-1	1	-1	1	-1	1	-1	1	1
	1	-1	1	1	-1	-1	1	-1	-1	1	-1	1	1	1
	2	0	-2	0	0	-2	0	2	0	0	0	0	-2	2
A ₁	2	0	2	0	0	0	0	0	2	0	-2	0	-2	-2
A ₂	2	0	2	0	0	0	0	0	-2	0	2	0	-2	-2
A ₃	2	0	-2	2	0	0	0	0	0	0	0	-2	2	-2
A ₄	2	0	-2	-2	0	0	0	0	0	0	0	2	2	-2

TABLE XI
CHARACTERS AT M

\underline{C}_1	\underline{C}_2	\underline{C}_3	\underline{C}_4	\underline{C}_5	\underline{C}_6	\underline{C}_7	\underline{C}_8	\underline{C}_9	\underline{C}_{10}	\underline{C}_{11}	\underline{C}_{12}	\underline{C}_{13}	\underline{C}_{14}	\underline{C}_{15}	\underline{C}_{16}	\underline{C}_{17}	\underline{C}_{18}	\underline{C}_{19}	\underline{C}_{20}
1	1	i	i	1	-1	-1	-i	-i	-1	1	1	i	i	1	-1	-1	-i	-i	-1
1	1	i	-i	-1	-1	-1	-i	i	1	1	1	i	-i	-1	-1	-1	-i	i	1
1	1	-i	i	-1	-1	-1	i	-i	1	1	1	-i	i	-1	-1	-1	i	-i	1
1	1	-i	-i	1	-1	-1	i	i	-1	1	1	-i	-i	1	-1	-1	i	i	-1
2	-2	0	0	0	-2	2	0	0	0	2	-2	0	0	0	-2	2	0	0	0
1	1	i	i	1	-1	-1	-i	-i	-1	-1	-1	-i	-i	-1	1	1	i	i	1
1	1	i	-i	-1	-1	-1	-i	i	1	-1	-1	-i	i	1	1	1	i	-i	-1
1	1	-i	i	-1	-1	-1	i	-i	1	-1	-1	i	-i	1	1	1	-i	i	-1
1	1	-i	-i	1	-1	-1	i	i	-1	-1	-1	i	i	-1	1	1	-i	-i	1
2	-2	0	0	0	-2	2	0	0	0	-2	2	0	0	0	2	-2	0	0	0

$\underline{C}_1 = E$	$\underline{C}_6 = Q$	$\underline{C}_{11} = J$	$\underline{C}_{16} = QJ$
$\underline{C}_2 = C_2$	$\underline{C}_7 = QC_2$	$\underline{C}_{12} = m_3$	$\underline{C}_{17} = Qm_3$
$\underline{C}_3 = TR_1 + TR_2$	$\underline{C}_8 = QTR_1 + QTR_2$	$\underline{C}_{13} = Tm_1 + Tm_2$	$\underline{C}_{18} = QTm_1 + QTm_2$
$\underline{C}_4 = TC_1 + TC_1^{-1}$	$\underline{C}_9 = QTC_1 + QTC_1^{-1}$	$\underline{C}_{14} = TJC_1 + TJC_1^{-1}$	$\underline{C}_{19} = QTJC_1 + QTJC_1^{-1}$
$\underline{C}_5 = R_1' + R_2'$	$\underline{C}_{10} = QR_1' + QR_2'$	$\underline{C}_{15} = m_1' + m_2'$	$\underline{C}_{20} = Qm_1' + Qm_2'$

About this notation: Have herein used the $D_{4h}^{1/4}$ point group notation and this may be correlated with past notation by:

$E = E$	$TC_1 = Tmm_2$	$J = J$	$TJC_1 = TmR_1$
$\underline{C}_2 = C_2$	$TC_1^{-1} = Tmm_1$	$m_3 = m_3$	$TJC_1^{-1} = TmR_2$
$TR_1 = Tmm_3$	$R_1' = R_1$	$Tm_1 = Tm$	$m_1' = m_1$
$TR_2 = TmJ$	$R_2' = R_2$	$Tm_2 = TmC_2$	$m_2' = m_2$

TABLE XII
CHARACTER SYSTEM AT X AND R

Symmetry Type	C_{-1}	C_{-2}	C_{-3}	C_{-4}	C_{-5}	C_{-6}	C_{-7}	C_{-8}	C_{-9}	C_{-10}
	1	1	1	1	1	1	1	1	1	1
	1	1	1	-1	-1	1	1	1	-1	-1
	1	1	-1	1	-1	1	1	-1	1	-1
	1	1	-1	-1	1	1	1	-1	-1	-1
	1	1	1	1	1	-1	-1	-1	-1	-1
	1	1	1	-1	-1	-1	-1	-1	1	1
	1	1	-1	1	-1	-1	-1	1	-1	1
	1	1	-1	-1	1	-1	-1	1	1	-1
X_1, R_1	2	-2	0	0	0	2	-2	0	0	0
X_2, R_2	2	-2	0	0	0	-2	2	0	0	0

TABLE XIII
CHARACTER SYSTEM FOR
THE POINT Λ

Symmetry Type	C_{-1}	C_{-2}	C_{-3}	C_{-4}	C_{-5}
1	1	1	1	1	1
2	1	1	1	-1	1
3	1	1	-1	1	-1
4	1	1	-1	-1	-1
5	2	-2	0	0	0

TABLE XIV
CHARACTER SYSTEM AT S,
 Σ , Δ , AND Y

Symmetry Type	C_{-1}	C_{-2}	C_{-3}	C_{-4}
1	1	1	1	1
2	1	1	-1	-1
3	1	-1	-1	1
4	1	-1	1	-1

TABLE XV
 REPRESENTATION APPLICABLE AT U, W, AND T

	<u>C₁</u>	<u>C₂</u>	<u>C₃</u>	<u>C₄</u>	<u>C₅</u>
U ₁	2	-2	0	0	0

TABLE XVI
 ALLOWED REPRESENTATIONS AT V

<u>C₁</u>	<u>C₂</u>	<u>C₃</u>	<u>C₄</u>	<u>C₅</u>	<u>C₆</u>	<u>C₇</u>	<u>C₈</u>	<u>C₉</u>	<u>C₁₀</u>
1	1	i	i	1	-1	-1	-i	-i	-1
1	1	i	-i	-i	-i	-1	-i	i	1
1	1	-i	i	-1	-1	-1	i	-i	1
1	1	-i	-i	1	-1	-1	i	i	-1
2	-2	0	0	0	-2	2	0	0	0

TABLE XVII
COMPATIBILITY RELATIONS

Γ_1	Γ_2	Γ_3	Γ_4	Γ_5	$\Gamma_{1'}$	$\Gamma_{2'}$	$\Gamma_{3'}$	$\Gamma_{4'}$	$\Gamma_{5'}$
Δ_1	Δ_2	Δ_1	Δ_2	$\Delta_3\Delta_4$	Δ_4	Δ_3	Δ_4	Δ_3	$\Delta_1\Delta_2$
Σ_1	Σ_3	Σ_3	Σ_1	$\Sigma_2\Delta_4$	Σ_4	Σ_2	Σ_2	Σ_4	$\Sigma_1\Sigma_3$
Λ_1	Λ_3	Λ_4	Λ_2	Λ_5	Λ_3	Λ_1	Λ_2	Λ_4	Λ_5

M_1	M_2	M_3	M_4	M_5	$M_{1'}$	$M_{2'}$	$M_{3'}$	$M_{4'}$	$M_{5'}$
Σ_1	Σ_3	Σ_3	Σ_1	$\Sigma_2\Sigma_4$	Σ_4	Σ_2	Σ_2	Σ_4	$\Sigma_1\Sigma_3$
V_1	V_2	V_3	V_4	V_5	V_3	V_4	V_1	V_2	V_5
Y_1	Y_1	Y_4	Y_4	Y_2Y_3	Y_3	Y_3	Y_2	Y_2	Y_1Y_4

X_1	X_2	R_1	R_2	Z_1	Z_2	Z_3	Z_4	A_1	A_2	A_3	A_4
$\Delta_1\Delta_2$	$\Delta_3\Delta_4$	W_1	W_1	$\Lambda_1\Lambda_2$	$\Lambda_3\Lambda_4$	Λ_5	Λ_5	V_1V_4	V_2V_3	V_5	V_5
W_1	W_1	U_1	U_1	U_1	U_1	U_1	U_1	T_1	T_1	T_1	T_1
Y_1Y_4	Y_2Y_3	T_1	T_1	S_1S_2	S_3S_4	S_1S_4	S_2S_3	S_1S_2	S_3S_4	S_1S_4	S_2S_3

APPENDIX B

DOUBLE GROUP ANALYSIS AND TIME REVERSAL

The treatment of the crystallographic double groups was initiated by the work of Bethe (79). His treatment gave consideration to the splitting of atomic states of half-integral quantum number J . Opechowski (80) was among the first to generalize this result so it could be used to represent spin orbit interactions in solids of a given periodicity. However, it remained for Elliot (81) to set down some definite rules for acquiring double group irreducible representations in terms of direct product representations.

Briefly, the method of considering spin-orbit interactions is to consider the fact that the spatial coordinates and the spin coordinates are quite distinct. Since there is no overlap between the two spaces, the double group may be considered in terms of a direct product representation of the two existent groups of operators. With this in mind, very distinct rules of combination may be extracted from the mathematical formulation of the group of ordered pairs. Using such a formulation, the additional representations for the stannic oxide space group were acquired and are given in Tables XIII through XXII. Table XXIII contains the necessary compatibility relations between these additional states.

Wigner (82) has demonstrated that extra degeneracies often occur because of time-reversal symmetry. The effects of time reversal can

be seen for three distinct cases depending upon the nature of the complex matrices D which form an irreducible representation of the group.

Following Elliot (81), these cases are:

- (a) D is real
- (b) D and D^* belong to inequivalent irreducible representations
- (c) D and D^* belong to equivalent representations but are distinct.

For electrons with spin Wigner has shown that for the various cases:

- (a) there is extra degeneracy and the representation D always occurs doubled
- (b) there is extra degeneracy and the representations D, D^* always occurs together
- (c) there is no extra degeneracy.

If there is no spin, rules (a) and (c) are reversed. Herring (83) has considered such problems for space groups and has developed a general criterion for determining the type of situation which will arise. Using his treatment, the concept of time reversal has been applied to the irreducible representations of the stannic oxide structure. For each wavevector group the type of time reversal degeneracy has been given in terms of (a), (b), or (c) for each irreducible representation. When type (b) occurs, it is of interest to determine which states are time reversal degenerate. Using the criterion set forth by Elliot (81), this may be done readily. Thus, each state of time reversal degeneracy type (b) has been further diagnosed by stating which two representations are equivalent.

TABLE XVIII

DOUBLE GROUP IRREDUCIBLE REPRESENTATIONS AT Γ

	\underline{C}_1	\underline{C}_2	\underline{C}_3	\underline{C}_4	\underline{C}_5	\underline{C}_6	\underline{C}_7	\underline{C}_8	\underline{C}_9	\underline{C}_{10}	\underline{C}_{11}	\underline{C}_{12}	\underline{C}_{13}	\underline{C}_{14}	TR
Γ_{1^+}	1	1	1	1	1	1	1	1	1	1	1	1	1	1	(a)
Γ_{2^+}	1	1	1	1	1	-1	-1	1	1	1	1	1	-1	-1	(a)
Γ_{3^+}	1	1	-1	-1	1	1	-1	1	1	-1	-1	1	1	-1	(a)
Γ_{4^+}	1	1	-1	-1	1	-1	1	1	1	-1	-1	1	-1	1	(a)
Γ_{5^+}	2	2	0	0	-2	0	0	2	2	0	0	-2	0	0	(a)
Γ_{6^+}	2	-2	$\sqrt{2}$	$-\sqrt{2}$	0	0	0	2	-2	$\sqrt{2}$	$-\sqrt{2}$	0	0	0	(c)
Γ_{7^+}	2	-2	$-\sqrt{2}$	$\sqrt{2}$	0	0	0	2	-2	$-\sqrt{2}$	$\sqrt{2}$	0	0	0	(c)
Γ_{6^-}	2	-2	$\sqrt{2}$	$-\sqrt{2}$	0	0	0	-2	2	$-\sqrt{2}$	$\sqrt{2}$	0	0	0	(c)
Γ_{7^-}	2	-2	$-\sqrt{2}$	$\sqrt{2}$	0	0	0	-2	2	$\sqrt{2}$	$-\sqrt{2}$	0	0	0	(c)
Γ_{1^-}	1	1	1	1	1	1	1	-1	-1	-1	-1	-1	-1	-1	(a)
Γ_{2^-}	1	1	1	1	1	-1	-1	-1	-1	-1	-1	-1	1	1	(a)
Γ_{3^-}	1	1	-1	-1	1	1	-1	-1	-1	1	1	-1	-1	1	(a)
Γ_{4^-}	1	1	-1	-1	1	-1	1	-1	-1	1	1	-1	1	-1	(a)
Γ_{5^-}	2	2	0	0	-2	0	0	-2	-2	0	0	2	0	0	(a)

$$\underline{C}_1 = E$$

$$\underline{C}_9 = \bar{J}$$

$$\underline{C}_2 = \bar{E}$$

$$\underline{C}_{10} = TmR_1 + TmR_2$$

$$\underline{C}_3 = Tmm_1 + Tmm_2$$

$$\underline{C}_{11} = Tm\bar{R}_1 + Tm\bar{R}_2$$

$$\underline{C}_4 = Tm\bar{m}_1 + Tm\bar{m}_2$$

$$\underline{C}_{12} = m_3 + \bar{m}_3$$

$$\underline{C}_5 = C_2 + \bar{C}_2$$

$$\underline{C}_{13} = Tm + TmC_2 + Tm\bar{m} + Tm\bar{C}_2$$

$$\underline{C}_6 = Tmm_3 + TmJ + Tm\bar{m}_3 + Tm\bar{J}$$

$$\underline{C}_{14} = m_1 + m_2 + \bar{m}_1 + \bar{m}_2$$

$$\underline{C}_7 = R_1' + R_2' + \bar{R}_1' + \bar{R}_2'$$

$$\underline{C}_8 = J$$

TABLE XIX
ADDITIONAL REPRESENTATIONS AT Γ

	\underline{C}_1	\underline{C}_2	\underline{C}_3	\underline{C}_4	\underline{C}_5	\underline{C}_6	\underline{C}_7	\underline{C}_8	\underline{C}_9	\underline{C}_{10}	\underline{C}_{11}	\underline{C}_{12}	\underline{C}_{13}	\underline{C}_{14}	TR
Γ_6^+	2	-2	$\sqrt{2}$	$-\sqrt{2}$	0	0	0	2	-2	$\sqrt{2}$	$-\sqrt{2}$	0	0	0	(c)
Γ_7^+	2	-2	$-\sqrt{2}$	$\sqrt{2}$	0	0	0	2	-2	$-\sqrt{2}$	$\sqrt{2}$	0	0	0	(c)
Γ_6^-	2	-2	$\sqrt{2}$	$-\sqrt{2}$	0	0	0	-2	2	$-\sqrt{2}$	$\sqrt{2}$	0	0	0	(c)
Γ_7^-	2	-2	$-\sqrt{2}$	$\sqrt{2}$	0	0	0	-2	2	$\sqrt{2}$	$-\sqrt{2}$	0	0	0	(c)

TABLE XX
ADDITIONAL REPRESENTATIONS AT A AND Z

64	Z_5	Same for A_5	Time Z	Reversal A
1	E	4	(c)	(c)
1	\bar{E}	-4		
1	Q	-4		
1	$Q\bar{E}$	4		
60 all others		0		

$E, \bar{E}, Q, Q\bar{E}, T(m_1+\bar{m}_1+m_2+\bar{m}_2) + QT(m_1+\bar{m}_1+m_2+\bar{m}_2), \underline{C}_2+\bar{C}_2, QR_1'+Q\bar{R}_1'+R_2'+\bar{R}_2',$
 $TC_1+QTC_1+QTC_1^{-1}+TC_1^{-1}, T\bar{C}_1+Q\bar{C}_1^{-1}+QTC_1+Q\bar{C}_1^{-1}, m_3+Qm_3+\bar{m}_3+Q\bar{m}_3, TR_1+\bar{R}_1+QT$
 $R_1+Q\bar{R}_1+TR_2+Q\bar{R}_2+\bar{R}_2+Q\bar{R}_2, J+QJ, \bar{J}+Q\bar{J}, m_1'+m_2'+\bar{m}_1'+\bar{m}_2', TJC_1+TJC_1^{-1}+QTJ$
 $\underline{C}_1+QTJC_1^{-1}, TJC_1+TJC_1^{-1}+QTJ\bar{C}_1+QTJ\bar{C}_1^{-1}, Qm_1'+Qm_2'+Q\bar{m}_1'+Q\bar{m}_2', R_1+\bar{R}_1+QR_2+Q$
 $\bar{R}_2, QC_2+Q\bar{R}_2$

TABLE XXI

ADDITIONAL REPRESENTATIONS AT Λ

	\underline{C}_1	\underline{C}_2	\underline{C}_3	\underline{C}_4	\underline{C}_5	\underline{C}_6	\underline{C}_7	
Λ_6	2	-2	$\sqrt{2}$	$-\sqrt{2}$	0	0	0	Type (a)
Λ_7	2	-2	$-\sqrt{2}$	$\sqrt{2}$	0	0	0	

$\underline{C}_1 = E, \underline{C}_2 = \bar{E}, \underline{C}_3 = T_{mm1} + T_{mm2}, \underline{C}_4 = \overline{T_{mm1}} + \overline{T_{mm2}}, \underline{C}_5 = C_2 + \bar{C}_2,$
 $\underline{C}_6 = T_m + T_m C_2 + \bar{T}_m + \bar{T}_m C_2$

TABLE XXII

ADDITIONAL REPRESENTATIONS AT Δ

	\underline{C}_1	\underline{C}_2	\underline{C}_3	\underline{C}_4	\underline{C}_5	
Δ_5	2	-2	0	0	0	Type (a)

$\underline{C}_1 = E, \underline{C}_2 = \bar{E}, \underline{C}_3 = T_m J + \overline{T_m J}, \underline{C}_4 = T_m C_2 + \overline{T_m C_2}, \underline{C}_5 = m_3 + \bar{m}_3$

TABLE XXIII

ADDITIONAL REPRESENTATIONS AT W, U, AND T

		Z_1	Z_2	Z_3	Z_4	
16						
1	(E 0)	1	1	1	1	Type (b)
1	(E t_{xy})	-1	-1	-1	-1	
2	($\mathcal{E}_{2z} 0$); ($\bar{\mathcal{E}}_{2z} t_{xy}$)	i	i	-i	-i	
2	($\mathcal{P}_x \tau$); ($\bar{\mathcal{P}}_x \tau+t_{xy}$)	i	-i	i	-i	
2	($\mathcal{P}_y \tau$); ($\bar{\mathcal{P}}_y \tau+t_{xy}$)	-1	1	1	-1	
8	(αa) x (z 0)	$\times [(\alpha a)]$				

W_1 & W_2 are time reversal degenerates as are W_3 , & W_4 . - $\underline{C}_1 = E, \underline{C}_2 = Q,$
 $\underline{C}_3 = C_2 + Q C_2, \underline{C}_4 = T_m + Q T_m, \underline{C}_5 = T_m C_2 + Q T_m C_2$: U_1 & U_3 , are time reversal degenerates as are U_2 & U_4 . - $\underline{C}_1 = E, \underline{C}_2 = Q, \underline{C}_3 = m_3 + Q m_3, \underline{C}_4 = T_m C_2 + Q T_m C_2, \underline{C}_5 = T_m J + Q T_m J$:

T_1 & T_3 are time reversal degenerates as are T_2 & T_4 . - $\underline{C}_1 = \{E|0\},$
 $\underline{C}_2 = \{E|Q\}, \underline{C}_3 = \{m_3|0, Q\}, \underline{C}_4 = \{m|\tau, \tau+Q\}, \underline{C}_5 = \{m m_3|\tau, \tau+Q\}.$

TABLE XXIV
 ADDITIONAL REPRESENTATIONS AT S, Σ , AND Y

Double Group Element	S_5, Σ_5	Double Group Elements	Y_5
E	2	E	2
\bar{E}	-2	\bar{E}	-2
$m_2 + \bar{m}_2$	0	$m_3 + \bar{m}_3$	0
$R_2 + \bar{R}_2$	0	$Tm + \bar{Tm}$	0
$m_3 + \bar{m}_3$	0	$Tmm_3 + \bar{Tmm}_3$	0

Time Reversal Types

Σ : Type (a)

S : Type (c)

Y : Type (c)

TABLE XXV

ADDITIONAL REPRESENTATIONS AND DOUBLE GROUP ELEMENTS AT X

Class	X_3	X_4
E	2	2
\bar{E}	-2	-2
Q	-2	-2
$Q\bar{E}$	2	2
C_2+QC_2	2i	-2i
\bar{C}_2+QC_2	-2i	2i
$TR_1+QTR_1+Q\bar{TR}_1+\bar{TR}_1$	0	0
$TR_2+QTR_2+Q\bar{TR}_2+\bar{TR}_2$	0	0
J+QJ	0	0
$\bar{J}+Q\bar{J}$	0	0
$m_3+\bar{m}_3$	0	0
$Qm_3+Q\bar{m}_3$	0	0
$Tm_1+\bar{Tm}_1+QTm_1+Q\bar{Tm}_1$	0	0
$Tm_2+\bar{Tm}_2+QTm_2+Q\bar{Tm}_2$	0	0

Type (b) X_3 and X_4 are Time Reversal Degenerate

TABLE XXVI

ADDITIONAL REPRESENTATIONS AND DOUBLE GROUP CLASSES AT R

	\underline{C}_1	\underline{C}_2	\underline{C}_3	\underline{C}_4	\underline{C}_5	\underline{C}_6	\underline{C}_7	\underline{C}_8	\underline{C}_9	\underline{C}_{10}	\underline{C}_{11}	\underline{C}_{12}	\underline{C}_{13}	\underline{C}_{14}	\underline{C}_{15}	\underline{C}_{16}	\underline{C}_{17}	\underline{C}_{18}	\underline{C}_{19}	\underline{C}_{20}	TR
R_3	1	-1	i	i	-1	-1	1	-i	-i	1	1	-1	i	i	-1	-1	1	-i	-i	1	b
R_4	1	-1	i	-i	1	-1	1	-i	i	-1	1	-1	i	-i	1	-1	1	-i	i	-1	b
R_5	1	-1	-i	i	1	-1	1	i	-i	-1	1	-1	-i	i	1	-1	1	i	-i	-1	b
R_6	1	-1	-i	-i	-1	-1	1	i	i	1	1	-1	-i	-i	-1	-1	1	i	i	1	b
R_7	1	-1	i	i	-1	-1	1	-i	-i	1	-1	1	-i	-i	1	1	-1	i	i	-1	b
R_8	1	-1	i	-i	1	-1	1	-i	i	-1	-1	1	-i	i	-1	1	-1	i	-i	1	b
R_9	i	-i	-i	i	1	-1	1	i	-i	-1	-1	1	i	-i	-1	1	-1	-i	i	1	b
R_{10}	i	-1	-i	-i	-1	-1	1	i	i	1	-1	1	i	i	1	1	-1	-i	-i	-1	b

$$\underline{C}_1 = E, \underline{C}_2 = Q, \underline{C}_3 = C_2 + Q\bar{C}_2, \underline{C}_4 = Tm_1 + QTm_1, \underline{C}_5 = Tm_2 + QTm_2, \underline{C}_6 = \bar{E}, \underline{C}_7 = Q\bar{E}, \underline{C}_8 = \bar{C}_2 + QC_2, \underline{C}_9 = Tm_1 + QTm_1, \underline{C}_{10} = Tm_2 + QTm_2$$

$$\underline{C}_{11} = J, \underline{C}_{12} = QJ, \underline{C}_{13} = m_3 + Qm_3, \underline{C}_{14} = TR_2 + QTR_2, \underline{C}_{15} = TR_1 + QTR_1, \underline{C}_{16} = \bar{J}, \underline{C}_{17} = Q\bar{J}, \underline{C}_{18} = m_3 + Qm_3, \underline{C}_{19} = TR_2 + QTR_2,$$

$$\underline{C}_{20} = TR_1 + QTR_1$$

Time Reversal Degenerate states (R_3, R_5); (R_4, R_6); (R_7, R_9); (R_8, R_{10})

TABLE XXVII

ADDITIONAL REPRESENTATIONS AND DOUBLE GROUP CLASSES AT M

	M_{11}	M_{12}	M_{13}	M_{14}
\underline{C}_1	2	2	2	2
\underline{C}_2	0	0	0	0
\underline{C}_3	0	0	0	0
\underline{C}_4	$\sqrt{2}i$	$-\sqrt{2}i$	$\sqrt{2}i$	$-\sqrt{2}i$
\underline{C}_5	$-\sqrt{2}i$	$\sqrt{2}i$	$-\sqrt{2}i$	$\sqrt{2}i$
\underline{C}_6	0	0	0	0
\underline{C}_7	-2	-2	-2	-2
\underline{C}_8	2	2	2	2
\underline{C}_9	0	0	0	0
\underline{C}_{10}	0	0	0	0
\underline{C}_{11}	$-\sqrt{2}i$	$\sqrt{2}i$	$-\sqrt{2}i$	$\sqrt{2}i$
\underline{C}_{12}	$\sqrt{2}i$	$-\sqrt{2}i$	$\sqrt{2}i$	$-\sqrt{2}i$
\underline{C}_{13}	0	0	0	0
\underline{C}_{14}	-2	-2	-2	-2
\underline{C}_{15}	2	2	-2	-2
\underline{C}_{16}	0	0	0	0
\underline{C}_{17}	0	0	0	0
\underline{C}_{18}	$\sqrt{2}i$	$-\sqrt{2}i$	$-\sqrt{2}i$	$\sqrt{2}i$
\underline{C}_{19}	$-\sqrt{2}i$	$\sqrt{2}i$	$\sqrt{2}i$	$-\sqrt{2}i$
\underline{C}_{20}	0	0	0	0

TABLE XXVII (CONT'D)

	M_{11}	M_{12}	M_{13}	M_{14}
\underline{C}_{21}	2	2	-2	-2
\underline{C}_{22}	0	0	0	0
\underline{C}_{23}	0	0	0	0
\underline{C}_{24}	$-\sqrt{2}i$	$\sqrt{2}i$	$\sqrt{2}i$	$-\sqrt{2}i$
\underline{C}_{25}	$\sqrt{2}i$	$-\sqrt{2}i$	$-\sqrt{2}i$	$\sqrt{2}i$
\underline{C}_{26}	0	0	0	0
\underline{C}_{27}	-2	-2	2	2
\underline{C}_{28}	-2	-2	2	2
TR	b	b	b	b

$$\underline{C}_1 = E, \underline{C}_2 = C_2 + \bar{C}_2, \underline{C}_3 = TR_1 + TR_2 + \bar{TR}_1 + \bar{TR}_2, \underline{C}_4 = Tm_1 + Tm_2,$$

$$\underline{C}_5 = Tm_1 + Tm_2, \underline{C}_6 = R_1 + R_2 + \bar{R}_1 + \bar{R}_2, \underline{C}_7 = Q, \underline{C}_8 = Q\bar{E},$$

$$\underline{C}_9 = QTm(m_3 + J + \bar{m}_3 + \bar{J}), \underline{C}_{10} = Q(C_2 + \bar{C}_2), \underline{C}_{11} = QTm(m_1 + m_2),$$

$$\underline{C}_{12} = QTm(\bar{m}_1 + \bar{m}_2), \underline{C}_{13} = QR_1 + R_2 + \bar{R}_1 + \bar{R}_2, \underline{C}_{14} = \bar{E}, \underline{C}_{15} = J,$$

$$\underline{C}_{16} = m_3 + \bar{m}_3, \underline{C}_{17} = Tm + TmC_2 + \bar{Tm} + \bar{Tm}C_2, \underline{C}_{18} = TmR_1 + TmR_2,$$

$$\underline{C}_{19} = Tm\bar{R}_1 + Tm\bar{R}_2, \underline{C}_{20} = m_1 + m_2 + \bar{m}_1 + \bar{m}_2, \underline{C}_{21} = QJ, \underline{C}_{22} = Q(m_3$$

$$+ \bar{m}_3), \underline{C}_{23} = QT(m + \bar{m} + mC_2 + \bar{m}C_2), \underline{C}_{24} = QT(mR_1 + mR_2), \underline{C}_{25} =$$

$$QT(\bar{m}R_1 + \bar{m}R_2), \underline{C}_{26} = Q(m_1 + m_2 + \bar{m}_1 + \bar{m}_2), \underline{C}_{27} = \bar{J}, \underline{C}_{28} = Q\bar{J}$$

Time Reversal Type b; Degenerate States: (11,12); (13,14)

TABLE XXVIII

ADDITIONAL REPRESENTATIONS AND DOUBLE GROUP CLASSES AT V

	\underline{C}_1	\underline{C}_2	\underline{C}_3	\underline{C}_4	\underline{C}_5	\underline{C}_6	\underline{C}_7	\underline{C}_8	\underline{C}_9	\underline{C}_{10}	\underline{C}_{11}	\underline{C}_{12}	\underline{C}_{13}	\underline{C}_{14}	T.R.
V_6	2	-2	$\sqrt{2}i$	$-\sqrt{2}i$	0	0	0	-2	2	$-\sqrt{2}i$	$\sqrt{2}i$	0	0	0	b
V_7	2	-2	$-\sqrt{2}i$	$\sqrt{2}i$	0	0	0	-2	2	$+\sqrt{2}i$	$-\sqrt{2}i$	0	0	0	b

$\underline{C}_1 = E, \underline{C}_2 = \bar{E}, \underline{C}_3 = T_{mm1} + T_{mm2}, \underline{C}_4 = T_{mm1} + T_{mm2}, \underline{C}_5 = T_m + T_m C_2 + T_m + T_m C_2, \underline{C}_6 = C_2 + \bar{C}_2$
 $\underline{C}_7 = m_1 + m_2 + \bar{m}_1 + \bar{m}_2, \underline{C}_i = Q C_{i-7} \text{ if } i > 7$

V_6 and V_7 are Time Reversal Degenerates

TABLE XXIX

COMPATIBLE ELECTRONIC STATES

(DOUBLE GROUP)

Γ_6^+	Γ_7^+	Γ_6^-	Γ_7^-	X_3	X_4	Z_5	A_5
Δ_5	Δ_5	Δ_5	Δ_5	Δ_5	Δ_5	$\Lambda_6 \Lambda_7$	$V_6 V_7$
Λ_6	Λ_7	Λ_6	Λ_7	$W_1 W_2$	$W_3 W_4$	$U_1 U_2 U_3 U_4$	$T_1 T_2 T_3 T_4$
Σ_5	Σ_5	Σ_5	Σ_5	Y_5	Y_5	$S_5 S_5$	$S_5 S_5$

R_3	R_4	R_5	R_6	R_7	R_8	R_9	R_{10}	M_{11}	M_{12}	M_{13}	M_{14}
W_2	W_3	W_4	W_5	W_2	W_3	W_4	W_5	5	5	5	5
U_2	U_3	U_4	U_5	U_2	U_3	U_4	U_5	Y_5	Y_5	Y_5	Y_5
T_2	T_3	T_4	T_5	T_2	T_3	T_4	T_5	V_6	V_7	V_6	V_7

APPENDIX C

OPTICAL SELECTION RULES

After the acquisition of the irreducible representations for the various wavevector groups, it is only natural to try to utilize these results to predict some further properties of the system. In particular, one may use a strictly group theoretical argument to predict the possible initial and final electron states for an electron that has been excited by radiation. For a completely general treatment of the possible selection rules applicable to a given crystal system the reader is referred to Lax and Hopfield (84). However, the simple treatment of the interaction of radiation with matter to stimulate direct transitions is quite straightforward in that the problem reduces to consideration of the integral:

$$\int (\psi^f(r,t))^* \psi(\text{Int}) \psi^i(r,t) d^3r$$

All Space

where ψ^f = final electron state, ψ^i = initial electron state and $\psi(\text{Int})$ represents the interaction being considered which stimulates the transition. If the integral is nonvanishing, the transition is allowed. However, a vanishing of the integral insures that the transition is at least first forbidden. Rather than performing this rather complicated integration, it is possible to extract the desired information simply by considering the nature of the interaction and the symmetry of initial and final electron states. In particular, for interaction with the

electromagnetic field, the interaction term must transform like a vector. This occurs since the electron-photon interaction is a vector interaction.

As a result of this idea, it is possible to determine which transitions are allowed simply by considering the direct product of the representations for the initial and final electron states with the representation within the group of the wavevector which transforms like a vector. After this direct product representation is broken into its irreducible sum, this sum must contain the most symmetric representation of the wavevector group or the transition is not allowed.

For the stannic oxide space group, there is no single representation which transforms like a vector. Instead, two different representations must be considered. The simple point group representation of the D_{4h}^{14} crystal system contains one doubly-degenerate representation which transforms like a vector in the x,y plane and another singly-degenerate representation which transforms like z. Thus, the entire interaction term must contain a sum of these two representations.

However, should one be interested in transitions that are energetically possible using radiation polarized parallel and perpendicular to the c-axis, it is evident that for polarization perpendicular to this axis, it is necessary to consider only the representation which transforms like (x,y). Similarly, for polarization parallel to this axis, only that representation which transforms like z is applicable.

With this in mind, the following set of tables have been constructed in which the possible initial and final electron states have been listed for each type of polarization. The classification of transitions for a random polarization of the incident radiation would require

that any one initial state could have many possible final states. Since this is the case, the set of final states may be acquired simply by considering all possible states allowed for any given initial state, i.e., since the sum of two irreducible representations are necessary to completely describe a vector interaction, the final states for such an interaction may be acquired by considering all states which result from summing the states due to both types of polarization.

Tables XXX through XXXIII give possible initial and final states which are indeed polarization dependent. As mentioned, the set of possible states for a random polarization may be seen to be that set of states acquired by considering both polarization types simultaneously.

TABLE XXX
OPTICAL SELECTION RULES AT Γ

Initial State	Allowed Final State	Initial State	Allowed Final State
$\Gamma_{2'}$ Interaction		$\Gamma_{5'}$ Interaction	
Γ_i	$\Gamma_i \times \Gamma_{2'}$	Γ_i	$\Gamma_i \times \Gamma_{5'}$
Γ_1	$\Gamma_{2'}$	Γ_1	$\Gamma_{5'}$
Γ_2	$\Gamma_{1'}$	Γ_2	$\Gamma_{5'}$
Γ_3	$\Gamma_{4'}$	Γ_3	$\Gamma_{5'}$
Γ_4	$\Gamma_{3'}$	Γ_4	$\Gamma_{5'}$
Γ_5	$\Gamma_{5'}$	Γ_5	$\Gamma_{1'} + \Gamma_{2'} + \Gamma_{3'} + \Gamma_{4'}$
$\Gamma_{1'}$	Γ_2	$\Gamma_{1'}$	Γ_5
$\Gamma_{2'}$	Γ_1	$\Gamma_{2'}$	Γ_5
$\Gamma_{3'}$	Γ_4	$\Gamma_{3'}$	Γ_5
$\Gamma_{4'}$	Γ_3	$\Gamma_{4'}$	Γ_5
$\Gamma_{5'}$	Γ_5	$\Gamma_{5'}$	$\Gamma_1 + \Gamma_2 + \Gamma_3 + \Gamma_4$

TABLE XXXI

POSSIBLE ALLOWED TRANSITIONS

Initial State	Final States	Initial State	Final States
Γ_1	$\Gamma_{2'} \text{ or } \Gamma_{5'} = (\Gamma_{2'}, \Gamma_{5'})$	$\Gamma_{1'}$	(Γ_2, Γ_5)
Γ_2	$(\Gamma_{1'}, \Gamma_{5'})$	$\Gamma_{2'}$	(Γ_1, Γ_5)
Γ_3	$(\Gamma_{4'}, \Gamma_{5'})$	$\Gamma_{3'}$	(Γ_4, Γ_5)
Γ_4	$(\Gamma_{3'}, \Gamma_{5'})$	$\Gamma_{4'}$	(Γ_3, Γ_5)
Γ_5	$(\Gamma_{1'}, \Gamma_{2'}, \Gamma_{3'}, \Gamma_{4'}, \Gamma_{5'})$	$\Gamma_{5'}$	$(\Gamma_1, \Gamma_2, \Gamma_3, \Gamma_4, \Gamma_5)$

TABLE XXXII

POSSIBLE ALLOWED TRANSITIONS AT Δ

Δ_i	$\Delta_i \times \Gamma_{2'}$	Δ_i	$\Delta_i \times \Gamma_{5'}$
Δ_1	Δ_3	Δ_1	$\Delta_1 + \Delta_2$
Δ_2	Δ_4	Δ_2	$\Delta_1 + \Delta_2$
Δ_3	Δ_1	Δ_3	$\Delta_3 + \Delta_4$
Δ_4	Δ_2	Δ_4	$\Delta_3 + \Delta_4$

Pertinent	Representations			
	\mathcal{C}_1	\mathcal{C}_2	\mathcal{C}_3	\mathcal{C}_4
$\Gamma_{2'}$	1	-1	-1	1
$\Gamma_{5'}$	2	2	0	0

Initial State	Possible Final State
Δ_1	$(\Delta_1, \Delta_2, \Delta_3)$
Δ_2	$(\Delta_1, \Delta_2, \Delta_4)$
Δ_3	$(\Delta_1, \Delta_3, \Delta_4)$
Δ_4	$(\Delta_2, \Delta_3, \Delta_4)$

TABLE XXXIII
 POSSIBLE ALLOWED TRANSITIONS AT λ

λ_i	$\lambda_i \times \Gamma_{2'}$	λ_i	$\lambda_i \times \Gamma_{5'}$
λ_1	λ_1	λ_1	λ_5
λ_2	λ_2	λ_2	λ_5
λ_3	λ_3	λ_3	λ_5
λ_4	λ_4	λ_4	λ_5
λ_5	λ_5	λ_5	$\lambda_1 + \lambda_2 + \lambda_3 + \lambda_4$

Initial State	Possible Final States
λ_1	(λ_1, λ_5)
λ_2	(λ_2, λ_5)
λ_3	(λ_3, λ_5)
λ_4	(λ_4, λ_5)
λ_5	$(\lambda_1, \lambda_2, \lambda_3, \lambda_4, \lambda_5)$

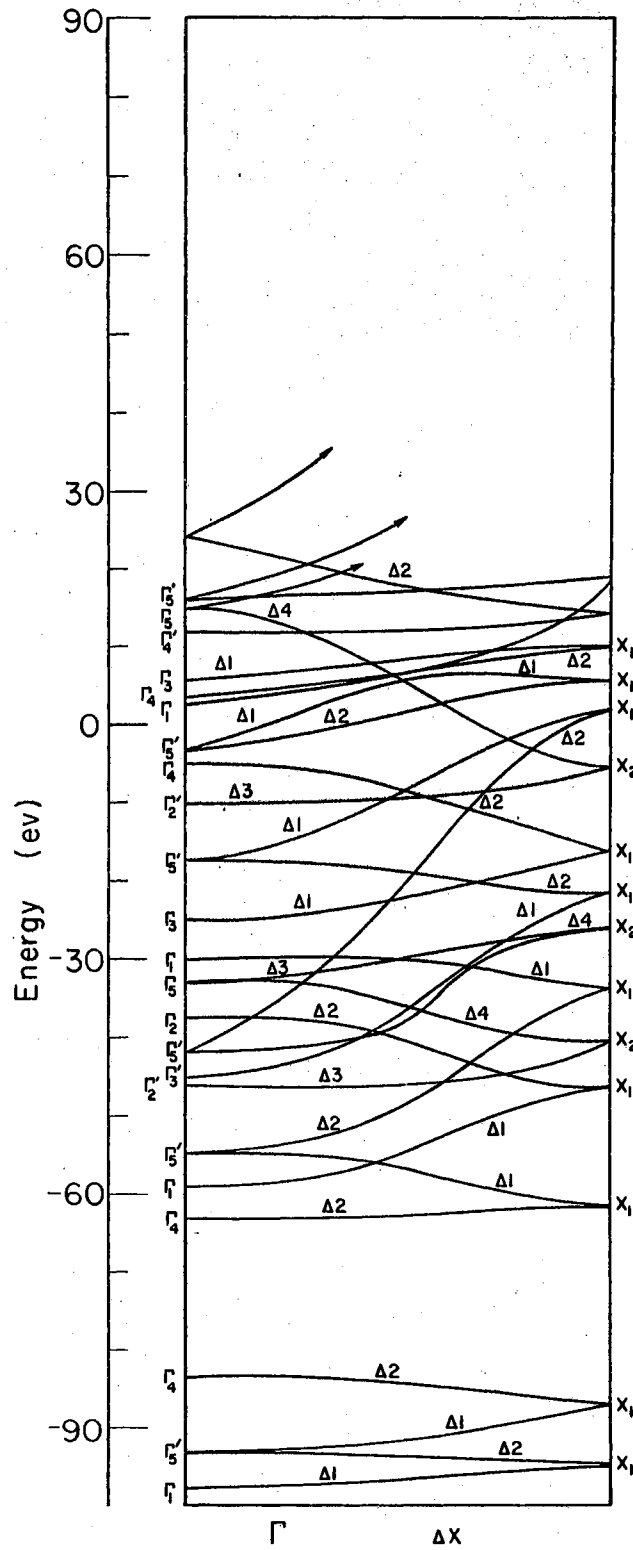


Figure 16. Pseudopotential Energy Bands Along the Axis $\Gamma-\Delta-X$

VITA

Bill P. Clark

Candidate for the Degree of
Doctor of Philosophy

Thesis: ULTRAVIOLET REFLECTIVITY AND BAND STRUCTURE OF STANNIC OXIDE

Major Field: Physics

Biographical:

Personal Data: Born in Bartlesville, Oklahoma, May 15, 1939, the son of Lloyd and Ruby Clark.

Education: Attended grade school in Bartlesville and Dewey, Oklahoma; and High School in Dewey, Oklahoma; received a Bachelor of Science degree from Oklahoma State University, Stillwater, Oklahoma, in May, 1961; received a Master of Science degree in May, 1964, from Oklahoma State University, Stillwater, Oklahoma; completed requirements for the Doctor of Philosophy degree in May, 1968.

Organizations: Member of Sigma Pi Sigma, Pi Mu Epsilon, American Physical Society, and the American Association for the Advancement of Science.